Aerosolization of Micro- and Nanoplastics via Sea Spray: Investigating the Role of Polymer Type, Size, and Concentration, and Potential Implications for Human Exposure

Authors: Silke Lambert[1,*], Maaike Vercauteren[1], Ana Isabel Catarino[2], Yunmeng Li[1,2], Josefien Van Landuyt[3], Nico Boon[3], Gert Everaert[2], Maarten De Rijcke[2], Colin R. Janssen [1,4], Jana Asselman[1]

***Corresponding author**

ORCIDs, emails:

- **Silke Lambert, 0000-0002-9680-3793,** Silke.Lambert@UGent.be
- **Maaike Vercauteren, 0000-0002-7618-143X ,** Maaike.vercauteren@ugent.be
- **Ana Isabel Catarino, 0000-0002-8796-0869,** ana.catarino@vliz.be
- **Yunmeng Li, 0000-0002-7660-1836,** yunmeng.li@vliz.be
- **Josefien Van Landuyt, 0000-0003-1611-1525,** josefien.vanlanduyt@ugent.be
- **Nico Boon, 0000-0002-7734-3103**, nico.boon@ugent.be
- **Gert Everaert, 0000-0003-4305-0617,** Gert.Everaert@vliz.be
- **Maarten De Rijcke, 0000-0002-0899-8122,** maarten.de.rijcke@vliz.be
- **Colin R. Janssen, 0000-0002-7781-6679,** colin.janssen@ugent.be
- **Jana Asselman, 0000-0003-0185-6516,** jana.asselman@ugent.be

Affiliations:

1. Blue Growth Research Lab, Ghent University, Wetenschapspark 1, Bluebridge 8400 Oostende, Belgium

2. Flanders Marine Institute (VLIZ), Research Department, Ocean and Human Health, InnovOcean Campus, Jacobsenstraat 1, 8400 Oostende, Belgium

3. Center for Microbial Ecology and Technology (CMET), Ghent University, Coupure Links 653, 9000 Ghent, Belgium

4. Ghent University Environmental Toxicology Lab (Ghentoxlab), Ghent University, Coupure Links 653, 9000 Ghent, Belgium

CRediT author statement:

Silke Lambert: Conceptualization, Investigation, Methodology, Validation, Formal analysis, Writing – original draft, Visualization, Writing –review & editing; **Maaike Vercauteren:** Conceptualization, Methodology, Validation, Supervision, Writing –original draft, Writing –review & editing; **Ana Isabel Catarino:** Conceptualization, Writing –review & editing; **Yunmeng Li:** Conceptualization, Writing – review & editing; **Josefien Van Landuyt:** Methodology; **Nico Boon**: Resources; **Gert Everaert:** Conceptualization, Writing –review & editing; **Maarten De Rijcke:** Conceptualization, Writing –review & editing; **Colin Janssen:** Conceptualization, Methodology, Resources, Writing –review & editing,

Funding acquisition; **Jana Asselman:** Conceptualization, Methodology, Resources, Supervision, Writing –original draft, Writing –review & editing, Funding acquisition

Reviewers:

- Dr Stephanie Wright, expert airborne plastic pollution. Faculty of Medicine, School of Public Health, Imperial College London, UK. s.wright19@imperial.ac.uk
- Dr Seung-Kyu Kim, expert in marine chemistry and marine pollution. Department of Marine Science, College of Natural Sciences, Incheon National University, Incheon, South Korea. skkim@inu.ac.kr
- Dr Deonie Allen, expert in microplastic atmospheric pollution. University of Strathclyde, Scotland, Uk. deonie.allen@strath.ac.uk
- Dr Alice Horton, Anthropogenic contaminants scientist with an expertise in microplastic pollution. National Oceanography Centre, UK. alihort@noc.ac.uk
- Dr Kimberly A. Prather, expert in marine ice nucleating particles. Department of Chemistry and Biochemistry, University of California, San Diego, USA. kprather@ucsd.edu
- Dr Filipa Bessa, expert in assessing the effects of (micro)plastic pollution on marine and coastal ecosystems. Coimbra University, Portugal. afbessa@uc.pt
- Ankush Kaushik, CSIR-National Institute of Oceanography, Dona Paula 403004, Goa, India
- Denise Mitrano, ETH Zürich, Dep. of Environmental Systems Science

Abstract

Micro- and nanoplastics (MNPs) can enter the atmosphere via sea spray aerosols (SSAs), but the effects of plastic characteristics on the aerosolization process are unclear. Furthermore, the importance of the transport of MNPs via these SSAs as a possible new exposure route for human health remains unknown. The aim of this study was two-fold: (1) to examine if a selection of factors affects aerosolization processes of MNPs, and (2) to estimate human exposure to MNPs via aerosols inhalation.

A laboratory-based bubble bursting mechanism, simulating the aerosolization process at sea, was used to investigate the influence of MNP as well as seawater characteristics. To determine the potential human exposure to microplastics via inhalation of SSAs, the results of the laboratory experiments were extrapolated to the field based on sea surface microplastic concentrations and the volume of inhaled aerosols.

Enrichment seemed to be influenced by MNP size, concentration and polymer type. With higher enrichment for smaller particles and denser polymers. Experiments with different concentrations showed a larger range of variability but nonetheless lower concentrations seemed to result in higher enrichment, presumably due to lower aggregation. In addition to the MNP characteristics, the type of seawater used seemed to influence the aerosolization process. Our human exposure estimate to microplastic via inhalation of sea spray aerosols shows that in comparison with reported inhaled concentrations in urban and indoor environments, this exposure route seems negligible for microplastics. Following the business-as-usual scenario on plastic production, the daily plastic inhalation in coastal areas in 2100 is estimated to increase but remain far below 1 particle per day.

This study shows that aerosolization of MNPs is a new plastic transport pathway to be considered, but in terms of human exposure it seems negligible compared to other more important sources of MNPs, based on current reported environmental concentrations.

Keywords: microplastics, nanoplastics, sea spray aerosols, atmosphere, human exposure, inhalation

Highlights

- Aerosolization increased with decreasing Polyethylene particle size
- Plastic concentration and polymer type influence plastic enrichment in aerosols
- Human plastic exposure via sea spray seems negligible compared to urban and indoor

1. Introduction

An increasing number of studies show that the sea acts as a reservoir for atmospheric microplastics (MPs), either through direct deposition of atmospheric MPs in the sea or through atmospheric fallout that enters the ocean via runoff (Dris et al., 2017). Liu et al. (2019) revealed that suspended atmospheric MPs, especially textile microfibers, are an important source of microplastic pollution in the ocean. Until recently, the sea has mostly been seen as a sink for atmospheric plastics, but the sea could also be a source for atmospheric micro- and nanoplastics. In addition to the long-range transport of particles from urban areas by wind, the ocean being a source of atmospheric MPs itself could be an explanation for the high concentrations of microplastics in remote uninhabited regions such as the Arctic (Bergmann et al., 2019). Brahney et al. (2021) suggest, based on modelling, that this pathway from ocean to air is responsible for 0 to 17% of the atmospheric microplastics in the USA. Among the hypothesized mechanisms, the transfer of plastic particles from the ocean to the air occurs via sea spray aerosols (SSAs) (Allen et al. 2020).

SSAs are formed when breaking waves cause bubbles of trapped air to rise to the surface and burst. This first step results in several hundreds of fine SSAs, which are called film drops. The burst bubble leaves a void behind that is filled again with water. This second step creates a water jet that produces larger SSAs, namely jet drops (Day, 1964; Blanchard, 1963). SSAs play a vital role in the Earth system, particularly in the interactions between atmosphere, biosphere, climate, and public health (Fröhlich-Nowoisky et al., 2016). Together with the SSAs particulate matter, microorganisms, fatty acids, carbohydrates, sterols, and proteins are aerosolized (Blanchard, 1963; Schiffer et al., 2018). For example, the study of Rastelli et al. (2017) indicated that SSAs were highly enriched in organic matter compared to the seawater samples. Also, DNA, viruses and prokaryotes were significantly enriched in SSAs (Pósfai et al., 2003). Furthermore, recent studies have shown that MNPs enter the atmosphere via SSAs (Catarino et al., 2023; Shiu et al., 2022; Yang et al., 2022). So, this could be an important transport pathway and an additional route for human exposure to MNPs. Exposure studies focused on inhalation have, until now, mainly focused on urban exposure, but the exposure via SSAs on the coastal inhabitants and tourists remains unclear.

Prior experimental evidence (Masry et al., 2021) has already indicated MNP particle transfer at the water-air interface through a bubble bursting method in controlled laboratory conditions. Aerosolization is a complex process dependent on characteristics of the water and substance. MNP size seemed to influence the aerosolization capacity as it was reported that smaller particles aerosolize better (Catarino et al., 2023). Next to size, the importance of factors such as MNP characteristics (e.g., polymer type) and concentration, that could influence the aerosolization, remain to be elucidated. Insight into these processes is essential to estimate the risk for human health and improve our understanding of this transport route. The aim of this study was, therefore, two-fold: (1) to examine if attributes such as polymer types, sizes and concentrations of MNPs and seawater affect the aerosolization process in an experimental setup, and (2) to estimate human exposure to microplastics via aerosols inhalation based on the results of the aforementioned experiments.

2. Materials and methods

2.1 Experimental setup

The experimental setup we used for mimicking the SSA formation was performed as per Masry et al. (2021). A schematic overview and detailed description can be found in SI A.1. To mimic the SSA formation, seawater was collected at sea (specified locations, section 2.4), transported and stored in a 10L plastic barrel, kept at 15 ± 1°C. All experiments were performed in an exposure room at a constant temperature of 15 ± 1°C. The seawater was added in a glass container and air was pumped through a sintered air stone at the bottom. The aerosols formed were caught on two types of filters placed in filter holders to capture both the aerosolized MNPs as well as aerosolized sodium (Na^+). Na^+ is used as a proxy to quantify SSA densities as it correlates directly to the amount of SSA (Lewis and Schwartz, 2004). MNPs were quantified using the cellulose nitrate filter (Whatman, diameter 47 mm, pore size of 0.8 µm or 0.2 µm; Table A.1) (Semmouri et al., 2023). Aerosolized Na^+ was quantified using the quartz filter (Whatman QM-A, diameter 47 mm, 2.2 µm pore size) as described in Van Acker et al. (2021b). Van Acker et al. (2021) showed that the quartz filter is suitable to collect aerosols and optimized the full SSA sampling method with quartz filters. The air supply through the air stone was 10 L/min or 5 L/min (depending on the series, see Table A.1) and was calibrated using a rotameter (SKC, Inc). Aerosols were collected on the filters using the Leland Legacy Sample Pumps (Cat. No. 100-3002; at 10 L/min) or 901-4011 SKC Flite4 sample

pumps (No. 22552498; at 5 L/min), depending on the series (Table A.1). Aerosols were collected for 24 hours during each experiment. At the end of the experiment, the total runtime (24 h) and the total volume of air pumped by each pump was verified to exclude any technical failures. The collected filters were stored in closed glass petri dishes and stored at 4 °C before further analysis. A thorough validation confirmed the setup to be suitable to study the aerosolization of MNPs in a controlled way. The filters' suitability to collect the aerosols was validated and the bubble sizes created in the setup were measured and compared with the bubble formation in the ocean (SI A.2).

Water samples were collected one hour after the experiment to compare the numbers of MNPs in the aerosols with the MNPs in the surface and bulk water. Samples of the surface layer and the water column were collected. For the samples of the surface layer (5 mL), a watch glass was placed just under the surface of the water and lifted vertically was described by Harvey and Burzell (1972). The water column samples (10 mL) were collected with a glass pipette. Three technical replicates of each water sample were taken: one replicate was used to analyze the sodium concentration, one replicate was used for the quantification of the plastics, and one replicate served as a spare sample. The water samples were stored at 4°C before further analysis.

To reduce contamination, the entire setup was cleaned thoroughly before the experiments using deionized water (Brander et al., 2020). Additionally, where possible, commercial colored MNPs were purchased (color range was selected based on the analysis technique) to be able to discriminate between contamination and added MNPs. The filter holders were dried, and the filters were placed inside the filter holders in a clean laminar flow cabinet, while a cotton lab coat was worn when preparing the filter holders. For every experiment, the setup was filled with fresh seawater and a new air stone as well as new plastic tubes were used. Airborne contamination was reduced as much as possible by storing all lab materials in a dust-free environment and by covering all cups, beakers and bottles with aluminum foil or with pre-rinsed watch glasses. Glass, metal or stainless-steel laboratory equipment was used when possible. Plastic tubing is used during the experiments, but blank experiments were performed to verify that these were not causing additional MNPs to be present.

2.2 Series of experiments

Four different series of experiments were set up, to study the influence of (1) MNP size, (2) polymer type, (3) MNP concentration and (4) seawater characteristics on the enrichment of plastics in sea spray aerosols. Experiments were repeated between 1 to 3 times. The general protocol of each experiment was similar. MNPs were added 24 h before the start of the aerosolization experiment to let the plastic particles distribute naturally in the seawater. As there were some minor differences between the experiments, mainly to enable analysis of different size classes of MNPs, an overview of all details of the experimental setup per experiment can be found in Table A.1 in SI. Blank experiments (negative controls) were performed in between the experiments. These blank experiments followed the exact same protocol without the addition of MNPs.

2.3 Microplastics and nanoplastics

Two polymer types were used: polyethylene (PE) and thermoset amino formaldehyde (TAF). TAF (1.3 g/cm^2) has a higher density than seawater and is used as a model for denser polymer types such as PET (1.38 g/cm^3) and PVC (1.38 g/cm^3). To resemble the variety in plastic pollution in the environment and understand how density may contribute to aerosolization, both floating and sinking polymers were tested. PE has a density lower than seawater (0.995 g/cm^3) and is used as a model for all buoyant polymer types such as PE and PP. Different sizes of MNPs were used ranging from nanoplastics to 27 µm plastic particles (Table A.1). In this study microplastics are defined as plastics between 1 and 5000 µm, and nanoplastics are all plastic particles smaller than 1 µm (Gigault et al., 2018). All MNPs solutions used are polydisperse, to maximize the environmental relevance of the results (Zimmermann et al., 2020). All used MNPs were characterized (Fourier-transform infrared spectroscopy (FTIR) spectra, scanning electron microscope (SEM) images and microscope measurements) of which the results can be found in SI A.

For experiments using PE (22-27 µm and 0.74-4.99 µm) and TAF (1-5 µm), plastic powders were weighted and added to the seawater. For the experiments using the nanoplastics (PE mostly <1 µm), a solution of cryo-milled PE particles was provided by the European Commission's Joint Research Center (JRC). The nanoplastics were dissolved in a water:methanol (1.33:1) solution, with 0.1% (v/v) TritonX. To remove the solvent and dispersant, the solution was centrifuged (5 min, 3500 RPM, 20 °C), the supernatant was removed and the nanoplastics were

dissolved in natural seawater. Nanosight characterization of the solution indicated that all particles are smaller than 5 µm and that 80% of them are smaller than 1 µm (SI A). The lower size limit of the experiment is 40 nm, based on the detection limit of the Nanosight, used to analyze the nanoplastics.

2.4 Seawater

Series 1 (except the nanoplastic experiments), 2 and 3 were performed using offshore seawater collected with the RV Simon Stevin, in collaboration with the Flanders Marine Institute (Belgium). The seawater was sampled using Niskin Bottles at station 330 (latitude 51° 25' 59.98", longitude 02° 48' 29.99") in the Belgian part of the North Sea, at a depth of 3 m on the 6th of December 2021. It is assumed that this type of seawater did not include the original sea surface microlayer (SSML) given the depth of sampling, as the SSML is defined as the uppermost 1-1000 µm layer (Wurl and Holmes, 2008). For the series 1 nanoplastic experiments, coastal seawater collected at a pier located in Ostend was used. This seawater was diluted using filtered near shore seawater from the Flanders Marine Institute (30 % coastal, 70 % filtered) to reach similar turbidity as the offshore seawater samples. In the experiment of series 4, coastal seawater collected at the beach in Ostend was used. It is assumed that this type of seawater did include the original SSML. Which type of seawater was used in which experiment is clearly stated in Table A.1.

2.5 Sample extraction and analysis

Plastic concentration

MNP concentrations were analyzed with different quantification techniques appropriate for their size, as no single technique was able to measure across this large range of particle sizes (SI A). All blanks underwent the exact same extraction and analytical procedure. To avoid contamination during the process, we adhered to the same guidelines as specified under the experimental setup. The largest particles, defined as PE 22-27 µm, were detected and quantified with the BX41 Olympus microscope directly from the cellulose nitrate filter. The water samples (surface and bulk) were filtered over cellulose nitrate filters and the filters were placed directly under the microscope. Images of a control sample (using the same type of filter and the same settings) were taken and based on these, a color threshold was set in Image J to differentiate the plastic particles from the filter background and other components. The color threshold, together with an additional visual inspection of every sample, was used to determine if microplastics were found on the filter.

For concentration measurements of particles between 0.74 and 5 µm in size, flow cytometry (Attune NxT Flow Cytometer, Thermo Fisher Scientific) was used. The cellulose nitrate filters were digested before analysis with 10 % KOH at 60 °C. The pH was corrected for the flow cytometer with HCl. As the flow cytometer can only analyze small volumes and high concentrations of particles, the samples were evaporated in the oven at 60 °C and dissolved in deionized water to increase the concentration. Finally, the samples were filtered over 20 µm filters to remove all big salt crystals that could lead to obstruction of the flow cytometer. The water samples (surface and bulk samples) were also evaporated and dissolved again in deionized water to increase the concentrations. For the flow cytometry analysis, the wells of a 96 well plate with a flat bottom were each filled with 200 µL of sample. For each sample replicate measurements were performed.

The already red fluorescent plastic particles did not need staining and were analyzed directly (at BL1 (530 nm) and RL1 (670 nm)). The non-fluorescent particles were stained first with Bodipy. The Bodipy 496/503 came from Invitrogen by Thermo Fischer Scientific (catalog code: D3922). A solution of 12.5 µg/mL of Bodipy dissolved in DMSO was created and 2 µL of this solution was added to each well and analyzed (at BL1 (530 nm) and BL3 (695 nm)). Positive control and negative control samples were measured together with the other samples. Control samples were also filtered over a 20 µm filter to make sure that this filter step, used in the preparation of the cellulose nitrate filter samples, does not remove any microplastics.

The data of the flow cytometer was analyzed using the flowCore package in R (Hahne et al., 2009). As there was no clear pattern observable in the data of the flow cytometer, defining a gating set was challenging. Hence, the mean value from the blank samples was subtracted from the results. This way other particles present in the seawater are subtracted from the results and also the noise created by the cellulose nitrate filters themselves is subtracted. This gave an indication of the number of microplastics present in the samples.

The smallest particles (nanoplastics) were measured using nanoparticle tracking analysis (Nanosight, Malvern type LM10). The cellulose nitrate filters were digested with 10 % KOH at 60 °C. For the water samples (surface

and bulk), no pretreatment was needed. For each measurement, one mL of the sample was sucked up. For each sample five replicate measurements were performed, each consisting of a video of 60 seconds. Based on these videos, five size distributions were generated that were combined into one general size distribution of each sample based on the mean and standard error of the five measurements.

To validate the reliability of the results, a second measurement was done of the samples of one replicate experiment. Different options were studied to determine the optimal settings for the analysis of these heterogeneous samples. The samples themselves were measured in fluorescence mode instead of scattering mode to try to only count the fluorescent plastic particles.

Sodium concentration

Na^+ was extracted from the quartz fiber filters and quantified, together with water samples, using inductively coupled plasma optical emission spectroscopy (ICP-OES) following the procedures in Van Acker et al. (2021b) (Supporting information A). Image analysis (Image J) was used to calculate the surface area used for Na^+ analysis and to recalculate the measured Na^+ mass for the full filter, assuming Na^+ is spread concentrically symmetrical. The total Na^+ mass is the sum of the Na^+ collected on the complete surface area of the filter, the Na^+ found in the first rinse of the filter holder and in the second rinse of the filter holder. The Na^+ mass from the blank filter and the blank reagent samples were deducted from the results to account for background Na^+ concentrations.

2.6 Calculation of enrichment factors

Data from the MNP and Na^+ analysis is used for the calculation of enrichment factors (EFs) using formulae by Van Acker et al. (2021b). The enrichment of MNPs in the SSAs and SSML is expressed as enrichment factors and is determined relative to Na^+. Na^+ is a common proxy to quantify SSA densities and is considered to have no enrichment (Lewis and Schwartz, 2004). That's why in the calculation of the enrichment factors, the sodium concentration is taken into account. Two types of EFs of MNPs were calculated namely the **[***EF***]***SSA* and the **[***EF***]***SSML*, following respectively Equations 1 and 2. The **[***EF***]***SSML* shows the enrichment of MNPs in the surface layer compared to the bulk water, while the **[***EF***]***SSA shows* the enrichment of MNPs in SSAs compared to the bulk water. Enrichment factors were compared in the different series of experiments in a descriptive manner.

$$EF(SSA) = \frac{\frac{[MNP]SSA}{[Na+]SSA}}{\frac{[MNP]bulk}{[Na+]bulk}} \text{ (Eq. 1)}$$

$$EF(SSML) = \frac{\frac{[MNP]SSML}{[Na+]SSML}}{\frac{[MNP]bulk}{[Na+]bulk}} \text{ (Eq. 2)}$$

[*MNP***]***SSA* is the number of aerosolized MNPs collected onto the cellulose nitrate filter per m^3 of air sampled (count/m^3). **[***Na+***]***SSA* is the amount of sodium collected onto the quartz filter per m^3 of air sampled (mg/m^3). **[***MNP***]***SSML* is the number of MNPs found in the surface layer sample (count/mL). **[***Na+***]***SSML* is the concentration of sodium found in the surface layer sample (mg/mL). **[***MNP***]***bulk* is the number of MNPs found in the water column sample (count/mL). **[***Na+***]***bulk* is the concentration of sodium found in the water column sample (mg/mL).

2.7 Estimate of human exposure to microplastics via inhalation

To determine the potential human exposure to microplastics via inhalation of SSAs, the results of the experiments in the lab were extrapolated to the field (detailed explanation in SI B.2). First, our results were recalculated to obtain a number of plastics per µg of Na^+, based on the number of microplastics and mass of Na^+ on the filters. For this, the data of the three replicate experiments with the TAF particles with a size of 1-5 µm are used. The focus is on particles between 1 and 5 µm as plastics smaller than 5 µm have the potential to reach the lungs (Jabbal et al., 2017; Lipworth et al., 2014). Nanoplastics (<1 µm) are excluded given the lack of reported environmental concentrations.

The environmental microplastic concentration data of Everaert et al. (2020) was used to obtain data on microplastic concentrations in the surface layer of the North Sea. An average was calculated from the concentrations in the North Sea area, expressed in plastic particles/m^3. The data was rescaled to cover the

microplastic size range from our experimental setup (from 1 µm-5 mm to 1 µm- 5 µm), based on the formula as described in Koelmans et al. (2020) and the most recent alfa value for marine surface water (alfa = 2.2) from Kooi et al. (2021). As it is predicted that the plastic concentrations in the ocean will keep increasing, a prediction of the future is made using the estimated plastic concentrations in 2050 and 2100 by Everaert et al. (2020).

Based on these rescaled environmental microplastic concentrations, an extrapolation of the aerosolization of microplastics in our lab experiments to aerosolization of microplastics in the North Sea was performed. This results into the number of microplastics that can be found per µg of Na^+ at the coast (*plastic in SSA*). To determine the number of microplastics that are inhaled by coastal populations, information is needed about the volume of SSAs in coastal air, Na^+ is used as a proxy for the volume of SSA. Van Acker et al. (2021a) measured the Na^+ concentrations in the air at the Belgian coast in a 1-year SSA sampling campaign (March 19, 2018 - March 19, 2019; 300 m from the waterline). The results of the SSA concentration range between 0.4 (minimum) and 6.3 (maximum) µg/m³. On average 1.8 µg/m³ was collected. An average inhalation rate of 20 m³ air/day was used based on Duarte-Davidson et al. (2001). This inhalation rate value is commonly used to determine the inhaled dose of a given air pollutant for adults. Walking at the coast thus gives an inhalation of 8 to 126 µg of SSAs per day, with an average of 36 µg of SSAs per day (*SSA rate*). Based on this data, the inhaled microplastics per day at the coast can be calculated using the following formula:

$$inhaled\ plastics\ [\#\ plastics/day] = plastic\ in\ SSA\ \left[\frac{\#\ plastics}{\mu g\ SSA}\right] * SSA\ rate\ \left[\frac{\mu g\ SSA}{day}\right]$$

3. Results

3.1 Enrichment factors

Series 1: Aerosolization in function of size with PE particles

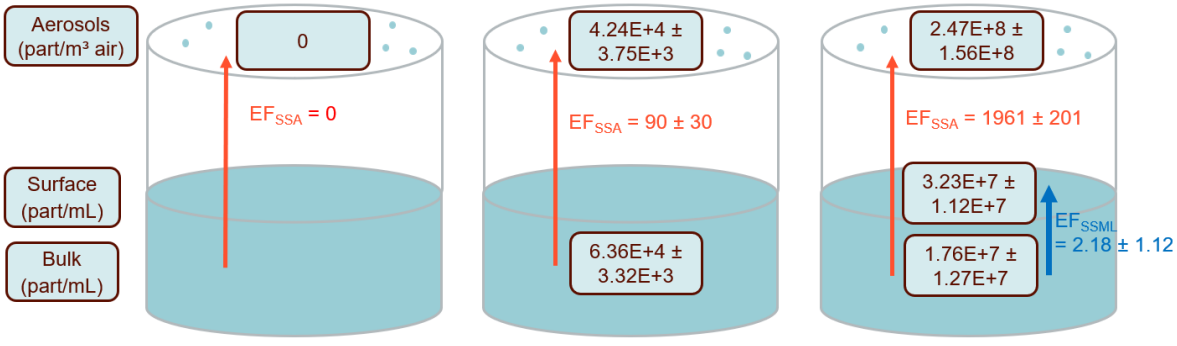

Figure 1: The mean (of the replicates) plastic concentrations in the bulk water samples, surface water samples and aerosol samples for three different sizes of PE particles. The red arrows show the mean enrichment factors of the sea spray aerosols (EF SSA) and the blue arrow shows the mean enrichment factor of the SSML. The EF SSML could not be calculated for every series. For the PE 0.74-4.99 µm particles, the mean [EF]SSA value of 90 ± 30. For replicate experiment 3, the number of particles was lower than the limit of detection and could not be used for the [EF]SSA. If a value of zero is taken for the [EF]SSA of experiment 3, the mean value for the PE 0.74-4.99 µm particles is 59 ± 56. If the limit of detection value is used in the calculation, the mean [EF]SSA becomes 69 ± 41. The mean value of the [EF]SSA will thus be between 59 and 90.

A size dependent effect was observed where the enrichment factors increased with decreasing size (Figure 1). No 22-27 µm plastics were found on the filters, meaning no aerosolization was observed for PE particles of 22-27 µm. 10^6 plastic particles were added to the experimental setup, but none were found on the filter: this leads to **[***EF***]***SSA* values which are zero. The PE particles of 0.74-4.99 µm were enriched in the aerosols with a mean **[***EF***]***SSA* value of 90 **±** 30. For replicate experiment 3, PE particles were found on the filter, but the number of particles was lower than the limit of detection and could not be used for the $[EF]_{SSA}$. If a value of zero is taken for the **[***EF***]***SSA* of experiment 3, the mean value for the PE 0.74-4.99 µm particles is 59 ± 56. If the limit of detection value is used in the calculation, the mean **[***EF***]***SSA* becomes 69 ± 41. The mean value of the **[***EF***]***SSA* will thus be between 59 and 90. The **[***EF***]***SSML* of these experiments could not be calculated as the concentration of PE particles in the surface water samples was under the detection limit and could thus not be trusted as results. For the experiments performed with the PE nanoparticles, the mean **[***EF***]***SSA* value is 1961 **±** 201. The mean

[*EF***]***SSML* is 2.18 **±** 1.12, indicating that the surface layer is enriched in nanoplastics compared to the bulk water, but the enrichment in the aerosols is a factor 1000 higher. The data used for the calculation of the enrichment factors can be found in Supporting information B.1.

Series 2: Aerosolization in function of polymer specific properties with PE and TAF particles

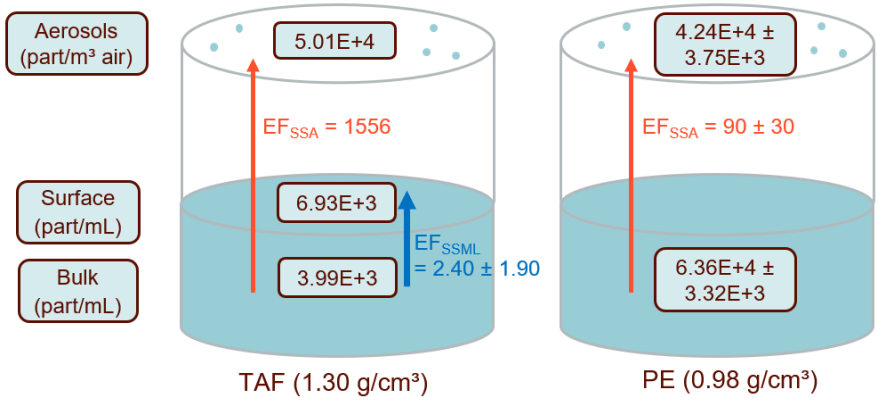

Figure 2: The mean (of the replicates) plastic concentrations in the bulk water samples, surface water samples and aerosol samples for two polymer types (TAF and PE). The red arrows show the mean enrichment factors of the sea spray aerosols (EF SSA) and the blue arrow shows the mean enrichment factor of the SSML. The EF SSML could not be calculated for every series. For the experiments performed with the TAF particles of 1-5 µm, the mean [EF]SSA value is 1556. For replicate experiments 1 and 2, the number of TAF particles found on the filters was lower than the detection limit and the [EF]SSA could thus not be calculated. If for both experiments, an [EF]SSA value of zero is considered, the mean [EF]SSA is 519. If the limit of detection value is used for the number of particles on the filters, the mean [EF]SSA becomes 759 ± 720. The mean [EF]SSA value will thus be between 519 and 1556.

The type of polymer had an impact of the enrichment factors as aerosolization was higher for the sinking particles (TAF) than for the floating particles (PE) (Figure 2). For the experiments performed with the PE particles of 0.74-4.99 µm, the results are the same as in series 1. For the experiments performed with the TAF particles of 1-5 µm, the mean **[***EF***]***SSA* value is 1556. For replicate experiments 1 and 2, particles were found, but the number of TAF particles found on the filters was lower than the detection limit and the **[***EF***]***SSA* could thus not be calculated. If for both experiments, an **[***EF***]***SSA* value of zero is considered, the mean **[***EF***]***SSA* is 519. If the limit of detection value is used for the number of particles on the filters, the mean **[***EF***]***SSA* becomes 759 **±** 720. The mean **[***EF***]***SSA* value will thus be between 519 and 1556. The mean **[***EF***]***SSML* is 2.4 **±** 1.9. This standard deviation is influenced by the outlier value of experiment 1. If this value is excluded a mean value of 1.3 **±** 0.53 is found. The [EF]*SSML* indicates that the surface layer contains twice as much microplastics compared to the bulk water, but the enrichment in the aerosols is more than a factor 500 higher. The data used for the calculation of the enrichment factors can be found in Supporting information B.1.

Series 3: Aerosolization in function of concentration

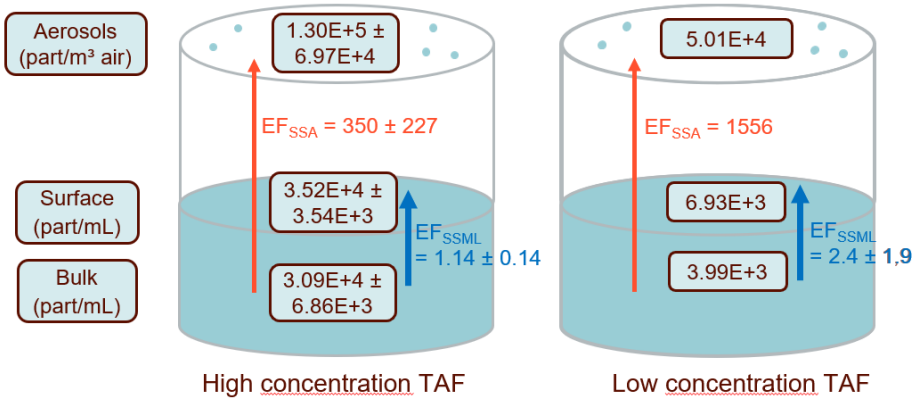

Figure 3: The mean (of the replicates) plastic concentrations in the bulk water samples, surface water samples and aerosol samples for two plastic concentrations of TAF particles. The red arrows show the mean enrichment factors of the sea spray aerosols (EF SSA) and the blue arrow shows the mean enrichment factor of the SSML. For the high concentration experiments 10^9 plastics were added, while in the low concentration experiments 10^6 plastic particles were added to the experimental

setup (800mL). For the experiments performed with the TAF particles of 1-5 µm, the mean [EF]SSA value is 1556. For replicate experiments 1 and 2, the number of TAF particles found on the filters was lower than the detection limit and the [EF]SSA could thus not be calculated. If for both experiments, an [EF]SSA value of zero is considered, the mean [EF]SSA is 519. If the limit of detection value is used for the number of particles on the filters, the mean [EF]SSA becomes 759 ± 720. The mean [EF]SSA value will thus be between 519 and 1556.

A concentration dependent effect was observed where the enrichment factor was higher if lower concentrations of microplastics were added (Figure 3). For the experiments performed with high concentrations of TAF the mean $[EF]_{SSA}$ value is 350 ± 227. The mean $[EF]_{SSML}$ is 1.14 ± 0.14, indicating only a small enrichment of microplastics in the surface layer compared to the bulk water. For the experiments performed with low concentrations of TAF, the data is the same as the TAF results of series 2 and thus ranges between 519 and 1556. The data used for the calculation of the enrichment factors can be found in SI B.1.

Series 4: Aerosolization in function of type of seawater

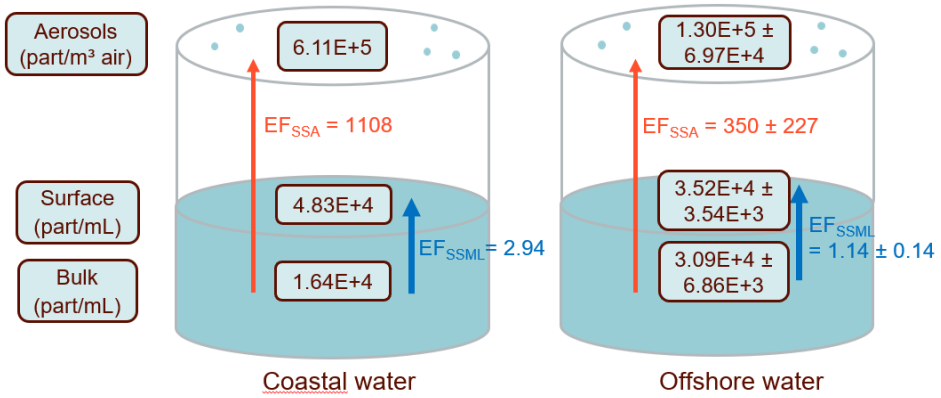

Figure 4: The mean (of the replicates) plastic concentrations in the bulk water samples, surface water samples and aerosol samples for two different seawater types: coastal water and offshore water. The tests were performed with TAF 1-5 µm particles. The red arrows show the mean enrichment factors of the sea spray aerosols (EF SSA) and the blue arrow shows the mean enrichment factor of the SSML.

A seawater dependent effect was observed (Figure 4): the enrichment factor was higher if coastal water (including the SSML) was used, compared to offshore water (without the SSML). The $[EF]_{SSA}$ of the experiment performed with coastal water that included the natural SSML layer is 1108, the $[EF]_{SSML}$ is 2.94. For the experiments performed with the same polymer type and size of microplastics, but with offshore seawater the mean $[EF]_{SSA}$ value is 350 ±227. The mean $[EF]_{SSML}$ is 1.14 ± 0.14. The $[EF]_{SSML}$ thus also indicates a higher enrichment of microplastics in the surface water when coastal water is used compared to offshore water. The data used for the calculation of the enrichment factors can be found in SI B.1.

3.2 Estimation of human exposure via inhalation

It was estimated that between 6.67 $x10^{-6}$ and 1.05 $x10^{-4}$ plastic particles with a size between 1 and 5 µm will be inhaled per day spend at the coast. With increasing plastic production and assumed increasing plastic pollution in time, the aerosolization is consequently assumed to increase as well. Nonetheless, even in 2100 in the business-as-usual scenario on plastic production, the estimated daily inhalation of microplastics with a size between 1 and 5µm is between 1.51 $x10^{-4}$ and 2.37 $x10^{-3}$ plastic particles/day (Figure 5). The intermediate results can be found in SI B.2.

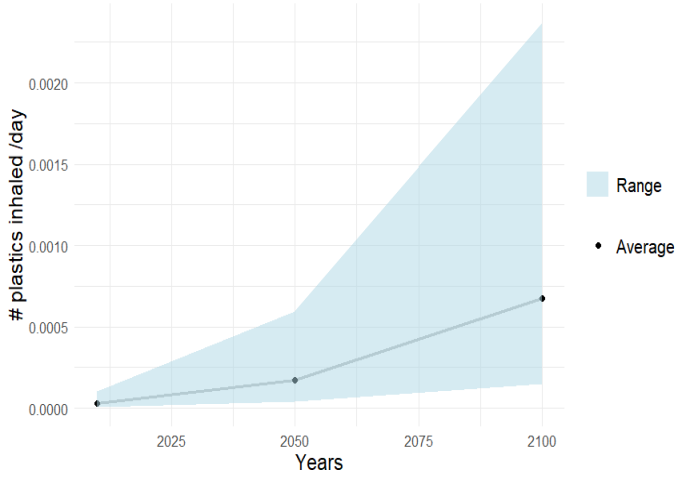

Figure 5: The number of plastics inhaled per day at the coast for 2010, 2050 and 2100. The range indicates the minimum and maximum values.

4. Discussion

The aerosolization of MNPs is a complex process that is influenced by different factors. To estimate the importance of this pathway for human exposure and aerosolization as an MNP transport route, the influence of these factors needs to be investigated. The results of this study highlight that all studied factors here, i.e. MNP characteristics (size, polymer type), concentration and the use of sea surface water, influence the aerosolization process.

Our data indicates that increasing MNP particle size resulted in decreasing aerosolization for PE particles. These results confirm the work of Catarino et al. (2023), showing a similar trend for 0.5, 1, 5, and 10 µm polystyrene particles. Harb et al. (2023) also showed a lower aerosolization for 10 µm PS particles compared to 2 µm particles. Masry et al. (2021) also showed a higher aerosolization for smaller particles but suggested that transfer is limited to particles smaller than 1 µm. The difference with our results can be attributed to the use of natural seawater in our study, while in the study of Masry et al. (2021) ultrapure water was used. In a field sampling study by Kaushik et al. (2024) microplastics in aerosols were reported between 20 µm to 5 mm. A hypothesis is that intense wave action in real ocean environments could cause larger particles to be ejected into the air compared to our experimental setup. In addition, in real environmental conditions, the transfer may depend on particle characteristics but also on the composition of the SSML, the types and concentrations of the present surfactants, as well as the salinity of the water. In future research, it would be useful to be able to measure the size distributions of the particles on the filters and in the water samples. This way, volume based instead of number-based enrichment factors could be calculated and it could be taken into account that within the size range tested, the smaller particles could aerosolize more than the bigger particles.

Second, we observed variability across different polymers. The sinking higher density polymer tested (TAF) showed a higher aerosolization than the floating lower density polymer (PE) tested. Harb et al. (2023) reported that floating PE particles are less effectively aerosolized than PS particles. They reported a significant number of PE aggregates that could be linked to a tendency of PE to aggregate more than PS due to surface properties. This might explain the lower aerosolization of PE particles, which also supports our first results indicating a link between size and aerosolization. It is important to note that in our experimental setup, the bubbles are coming from the bottom. As the denser TAF particles tend to sink, these particles could be taken with the bubbles and interact stronger with the bubbles compared to where a plunging jet might actually partially push them down. In the real environment, different upward and downward forces will act on the particles (gravitational settling, turbulence, the seawater lapping at the surface, currents, …) and this is not taken into account in our experimental setup. These forces indicate that factors beyond density affect the transport of these materials, potentially leading to their enrichment in the SSML. These results might thus be dependent on the experimental setup used and can be different in real environmental conditions. More research is needed to understand the role of the chemical polymer composition on aerosolization. In addition to the density, other polymer

characteristics like hydrophobicity and morphology could have an effect on the aerosolization process and need to be investigated in the future. In this study, we did not distinguish between these specific characteristics.

Third, we suggest an effect of concentration. Lower concentrations of microplastics can result in a higher enrichment. A likely reasoning is particle aggregation upon higher concentrations. Wang et al. (2021) showed that aggregation of microplastics is an important physicochemical process dominating the transport behavior and overall fate of microplastics in aquatic environments. This aggregation can occur between microplastics (homoaggregation) or between microplastics and different types of particles (like organisms and organic material) (heteroaggregation). This potential aggregation of microplastics in natural seawater might be a reason for the lower aerosolization at a higher microplastic concentration, as also suggested by Harb et al. (2023). Due to the lower environmental MNP concentrations, mostly heteroaggregation is expected in the field, while in our experimental setup higher concentrations of plastics are used, possibly also resulting in homoaggregation. Other studies also show a higher enrichment in the SSML if the concentrations in the bulk seawater are lower. Higher enrichment was observed for DOC and POC in the SSML, when low concentrations were present in the bulk seawater (van Pinxteren et al., 2012; van Pinxteren et al., 2017). The average EF SSA for TAF 1-5 µm low concentrations is in the range between 519 and 1556. The three experiments show a high variability in EF SSA values. For low concentrations, it can depend on the spatial location of the low number of particles, if they are incorporated in the aerosols. This spatial variation is likely higher at lower concentrations then at higher concentrations leading to more variation in the EF in low concentrations versus high concentration where particles are likely more homogenously distributed. This could result in a large variation of number of particles in the aerosols and thus in the EF SSA. Further research is needed with realistic polymer mixtures in realistic concentrations, which include among others other natural particles.

Fourth, seawater characteristics affect the aerosolization process. Here, we compared natural seawater collected in two ways. Offshore seawater is taken at a depth of 3 m, so no natural SSML layer was sampled. The water taken at the coast included the natural SSML. Our results indicate that the coastal water, with the SSML included, contributes to higher aerosolization of microplastics. The SSML can namely be enriched with organic matter, bioactive molecules, organisms and surfactants, which could influence the aerosolization process (Casas et al., 2020; Flores et al., 2021; Lv et al., 2020). The biogenic surfactant dipalmitoylphosphatidylcholine (DPPC), is for example known to accumulate in the SSML (Van Acker et al., 2021a). In general, the use of natural seawater compared to artificial seawater in aerosolization experiments is suggested to have an effect. Studies using artificial seawater (Catarino et al., 2023; Shiu et al., 2022) showed much lower enrichment factors. Catarino et al. (2023) expects that the presence of microorganisms in the SSML will augment the enrichment factors for MNPs. Yang et al. (2022) on the other hand suggested in their experiments that microplastic transfer processes with natural seawater can be realistically reproduced with synthetic seawater. They, however, filtered the natural seawater over 4.5 µm, removing a lot of the microorganisms. This filtering step will affect the SSML composition and the aerosolization process. Further research is thus needed to elucidate how the biochemical composition of the SSML and seawater in general influences aerosolization.

The MNPs in sea spray aerosols can be inhaled by coastal populations. However, it is unclear how much this pathway contributes to the human exposure to MNPs via inhalation. Here, we made a first step to assess potential human exposure by extrapolating results from the laboratory setting to field. Our first estimate showed that between 6.67 $x10^{-6}$ and 1.05 $x10^{-4}$ plastic particles with a size between 1 and 5 µm will be inhaled per day spend at the coast. This is negligible compared to reported inhalation exposure in urban context where estimates showed an inhalation of 1.5 particles per m^3 and indoor, where even higher concentrations of 60 particles per m^3 are inhaled (UN, 2021). Our results show a large variation due to the weather influence on the number of aerosols formed. With increasing plastic production and assumed plastic pollution over time, the aerosolization is consequently assumed to increase as well. Nonetheless, following the business-as-usual scenario on plastic production, the daily inhalation in 2100 via SSAs of 1-5 µm microplastics is estimated to still be far below 1 particle per day. Furthermore, both urban and indoor particle pollution will similarly increase under the business-as-usual scenario. Based on our first estimate, sea spray aerosols might not relevantly contribute to the total plastic exposure concentration by inhalation.

In most plastic-aerosol experiments (including our experiment) MNP concentrations of 10^4-10^6 particles/mL are used (Shiu et al., 2021; Yang et al., 2022). Higher MNP concentrations are used in the experiments than in the real ocean situation (18 particles/m^3 in 2010, see SI B.2). This is because the concentrations need to be high enough for analytical detection limits. The results of series 3 show that lower concentrations of microplastics result in higher aerosolization levels for TAF particles, but this could thus not be taken into account in the extrapolation. To be able to take concentration into account, concentration response curves are crucial to determine the relationship between the concentration in the water and the number of plastics in the aerosols. Currently, due to the lack of environmental concentrations of nanoplastics and a lack of knowledge on how they behave, it is impossible to do a similar extrapolation for nanoplastics.

Although aerosolization of MNPs via sea spray aerosols might not relevantly contribute to human microplastic exposure via inhalation, this process is still important to take into account in the source- sink dynamics of the plastic cycle (Bank, M. S., & Hansson, S. V.; 2019). Indeed, the ocean is not only a sink for MNPs but also a source. This process also contributes to understanding the plastic fluxes to remote regions (Bergmann et al., 2019; Allen et al., 2019). Furthermore, marine aerosols play a vital role in the Earth system and influence the radiation balance of the Earth by scattering and absorbing solar radiation (Rastelli et al., 2017; Schiffer et al., 2018). The potential impact of the presence of MNPs in these aerosols remains to be elucidated.

Conclusion

This study investigated the transfer of MNPs to the atmosphere via SSAs. The results showed that aerosolization of MNPs is influenced by multiple factors including size, polymer type, concentration and composition of the seawater. Future research on MNP aerosolization should thus take these different factors into account to resemble realistic plastic pollution situations. A first estimate of human exposure to microplastics via the inhalation of SSAs shows that this pathway is negligible for human exposure compared to exposure to microplastics in outdoor urban environments and indoor air. An increase of the exposure of microplastics via SSAs is expected in the future due to increasing plastic pollution. This study shows that aerosolization is a new plastic transport pathway to take into account, but that human exposure to microplastics via SSAs seems negligible compared with other sources.

Acknowledgement

We would like to thank JRC for providing the plastics used for the experiments. We would like to thank Nancy De Saeyer, Noëmi Rogiers and Miao Peng for the help during the experiments. This work was supported by the Ghent University Research Fund (BOFSTG2020001201) awarded to Jana Asselman and the postdoctoral fellowship (BOF_PDO_01P08121) awarded to Maaike Vercauteren.

Competing interest

No competing interest.

References

Allen, S., Allen, D., Moss, K., Le Roux, G., Phoenix, V. R., and Sonke, J. E. (2020). Examination of the ocean as a source for atmospheric microplastics. *PloS one*, *15*(5), e0232746. https://doi.org/10.1371/journal.pone.0232746

Allen, S., Allen, D., Phoenix, V. R., Le Roux, G., Jiménez, P. D., Simonneau, A., Binet, S., and Galop, D. (2019). Atmospheric transport and deposition of microplastics in a remote mountain catchment. *Nature Geoscience*, *12*(5), 339–344. https://doi.org/10.1038/s41561-019-0335-5

Bank, M. S., & Hansson, S. V. (2019). The plastic cycle: a novel and holistic paradigm for the anthropocene. *Environmental Science & Technology*, *53*(13), 7177–7179. https://doi.org/10.1021/acs.est.9b02942

Bergmann, M., Mützel, S., Primpke, S., Tekman, M. B., Trachsel, J., and Gerdts, G. (2019). White and wonderful? microplastics prevail in snow from the alps to the arctic. *Science advances*, *5*(8), eaax1157. https://doi.org/10.1126%2Fsciadv.aax1157

Blanchard, D. C. (1963). The electrification of the atmosphere by particles from bubbles in the sea. *Progress in oceanography*, *1*, 73-202. https://doi.org/10.1016/0079-6611(63)90004-1

Brahney, J., Mahowald, N., Prank, M., Cornwell, G., Klimont, Z., Matsui, H., and Prather, K. A. (2021). Constraining the atmospheric limb of the plastic cycle. *Proceedings of the National Academy of Sciences*, *118*(16), e2020719118. https://doi.org/10.1073/pnas.2020719118

Brander, S. M., Renick, V. C., Foley, M. M., Steele, C., Woo, M., Lusher, A., ... & Rochman, C. M. (2020). Sampling and quality assurance and quality control: a guide for scientists investigating the occurrence of microplastics across matrices. *Applied Spectroscopy*, *74*(9), 1099-1125. https://doi.org/10.1177/0003702820945713

Casas, G., Martínez-Varela, A., Roscales, J. L., Vila-Costa, M., Dachs, J., and Jiménez, B. (2020). Enrichment of perfluoroalkyl substances in the sea-surface microlayer and seaspray aerosols in the southern ocean. *Environmental Pollution*, *267*, 115512. https://doi.org/10.1016/j.envpol.2020.115512

Catarino, A. I., León, M. C., Li, Y., Lambert, S., Vercauteren, M., Asselman, J., ... & De Rijcke, M. (2023). Micro-and nanoplastics transfer from seawater to the atmosphere through aerosolization under controlled laboratory conditions. *Marine Pollution Bulletin*, *192*, 115015. http://doi.org/10.1016/j.marpolbul.2023.115015

Day, J. A. (1964). Production of droplets and salt nuclei by the bursting of air-bubble films. *Quarterly Journal of the Royal Meteorological Society*, *90*(383), 72-78. https://doi.org/10.1002/qj.49709038307

Dris, R., Gasperi, J., Mirande, C., Mandin, C., Guerrouache, M., Langlois, V., and Tassin, B. (2017). A first overview of textile fibers, including microplastics, in indoor and outdoor environments. *Environmental pollution*, *221*, 453–458. https://doi.org/10.1016/j.envpol.2016.12.013

Duarte-Davidson, R., Courage, C., Rushton, L., & Levy, L. (2001). Benzene in the environment: an assessment of the potential risks to the health of the population. *Occupational and environmental medicine*, *58*(1), 2-13. https://doi.org/10.1136/oem.58.1.2

Everaert, G., De Rijcke, M., Lonneville, B., Janssen, C. R., Backhaus, T., Mees, J., ... & Vandegehuchte, M. B. (2020). Risks of floating microplastic in the global ocean. *Environmental Pollution*, *267*, 115499. https://doi.org/10.1016/j.envpol.2020.115499

Flores, J. M., Bourdin, G., Kostinski, A. B., Altaratz, O., Dagan, G., Lombard, F., Haëntjens, N., Boss, E., Sullivan, M. B., Gorsky, G., et al. (2021). Diel cycle of sea spray aerosol concentration. *Nature communications*, *12*(1), 1–12. https://doi.org/10.1038/s41467-021-25579-3

Fröhlich-Nowoisky, J., Kampf, C. J., Weber, B., Huffman, J. A., Pöhlker, C., Andreae, M. O., Lang-Yona, N., Burrows, S. M., Gunthe, S. S., Elbert, W., et al. (2016). Bioaerosols in the earth system: Climate, health, and ecosystem interactions. *Atmospheric Research*, *182*, 346–376. https://doi.org/10.1016/j.atmosres.2016.07.018

Gigault, J., Ter Halle, A., Baudrimont, M., Pascal, P. Y., Gauffre, F., Phi, T. L., ... & Reynaud, S. (2018). Current opinion: what is a nanoplastic?. *Environmental pollution, 235*, 1030-1034. https://doi.org/10.1016/j.envpol.2018.01.024

Hahne, F., LeMeur, N., Brinkman, R. R., Ellis, B., Haaland, P., Sarkar, D., ... & Gentleman, R. (2009). flowCore: a Bioconductor package for high throughput flow cytometry. *BMC bioinformatics*, *10*(1), 1-8. https://doi.org/10.1186/1471-2105-10-106

Harb, C., Pokhrel, N., & Foroutan, H. (2023). Quantification of the Emission of Atmospheric Microplastics and Nanoplastics via Sea Spray. *Environmental Science & Technology Letters*, *10*(6), 513–519. https://doi.org/10.1021/acs.estlett.3c00164

Harvey, G. W. and Burzell, L. A. (1972). A simple microlayer method for small samples 1. *Limnology and Oceanography*, *17*(1), 156–157. https://doi.org/10.4319/lo.1972.17.1.0156

Jabbal, S., Poli, G., & Lipworth, B. (2017). Does size really matter?: Relationship of particle size to lung deposition and exhaled fraction. *Journal of Allergy and Clinical Immunology*, *139*(6), 2013-2014. https://doi.org/10.1016/j.jaci.2016.11.036

Kaushik, A., Gupta, P., Kumar, A., Saha, M., Varghese, E., Shukla, G., ... & Gunthe, S. S. (2024). Identification and physico-chemical characterization of microplastics in marine aerosols over the northeast Arabian Sea. *Science of The Total Environment*, *912*, 168705. https://doi.org/10.1016/j.scitotenv.2023.168705

Koelmans, A. A., Redondo-Hasselerharm, P. E., Mohamed Nor, N. H., & Kooi, M. (2020). Solving the nonalignment of methods and approaches used in microplastic research to consistently characterize risk. *Environmental science & technology*, *54*(19), 12307-12315. https://doi.org/10.1021/acs.est.0c02982

Kooi, M., Primpke, S., Mintenig, S. M., Lorenz, C., Gerdts, G., & Koelmans, A. A. (2021). Characterizing the multidimensionality of microplastics across environmental compartments. *Water Research*, *202*, 117429. https://doi.org/10.1016/j.watres.2021.117429

Lipworth, B., Manoharan, A., & Anderson, W. (2014). Unlocking the quiet zone: the small airway asthma phenotype. *The Lancet Respiratory Medicine*, *2*(6), 497-506. https://doi.org/10.1016/s2213-2600(14)70103-1

Liu, K., Wu, T., Wang, X., Song, Z., Zong, C., Wei, N., and Li, D. (2019). Consistent transport of terrestrial microplastics to the ocean through atmosphere. *Environmental science technology*, *53*(18), 10612–10619. https://doi.org/10.1021/acs.est.9b03427

Lv, C., Tsona, N. T., and Du, L. (2020). Sea spray aerosol formation: results on the role of different parameters and organic concentrations from bubble bursting experiments. *Chemosphere*, *252*, 126456. https://doi.org/10.1016/j.chemosphere.2020.126456

Masry, M., Rossignol, S., Roussel, B. T., Bourgogne, D., Bussière, P.-O., R'mili, B., and Wong- Wah-Chung, P. (2021). Experimental evidence of plastic particles transfer at the water-air interface through bubble bursting. *Environmental Pollution*, *280*, 116949. https://doi.org/10.1016/j.envpol.2021.116949

Pósfai, M., Li, J., Anderson, J. R., and Buseck, P. R. (2003). Aerosol bacteria over the southern ocean during ace-1. *Atmospheric Research*, *66*(4), 231–240. https://doi.org/10.1016/S0169-8095(03)00039-5

Rastelli, E., Corinaldesi, C., Dell'Anno, A., Martire, M. L., Greco, S., Facchini, M. C., Rinaldi, M., O'Dowd, C., Ceburnis, D., and Danovaro, R. (2017). Transfer of labile organic matter and microbes from the ocean surface to the marine aerosol: an experimental approach. *Scientific reports*, *7*(1), 1–10. https://doi.org/10.1038/s41598-017-10563-z

Schiffer, J. M., Mael, L. E., Prather, K. A., Amaro, R. E., & Grassian, V. H. (2018). Sea spray aerosol: Where marine biology meets atmospheric chemistry. *ACS central science*, *4*(12), 1617-1623. https://doi.org/10.1021/acscentsci.8b00674

Semmouri, I., Vercauteren, M., Van Acker, E., Pequeur, E., Asselman, J., & Janssen, C. (2023). Distribution of microplastics in freshwater systems in an urbanized region: A case study in Flanders (Belgium). *Science of The Total Environment*, *872*, 162192. http://dx.doi.org/10.1016/j.scitotenv.2023.162192

Shiu, R. F., Chen, L. Y., Lee, H. J., Gong, G. C., & Lee, C. (2022). New insights into the role of marine plastic-gels in microplastic transfer from water to the atmosphere via bubble bursting. *Water Research*, *222*, 118856. https://doi.org/10.1016/j.watres.2022.118856

United Nations Environment Programme (2021). From Pollution to Solution: A global assessment of marine litter and plastic pollution. ISBN: 978-92-807-3881-0

Van Acker, E., De Rijcke, M., Liu, Z., Asselman, J., De Schamphelaere, K. A., Vanhaecke, L., and Janssen, C. R. (2021a). Sea spray aerosols contain the major component of human lung surfactant. *Environmental science & technology, 55*(23), 15989-16000. http://doi.org/10.1021/acs.est.1c04075

Van Acker, E., Huysman, S., De Rijcke, M., Asselman, J., De Schamphelaere, K. A., Vanhaecke, L., and Janssen, C. R. (2021b). Phycotoxin-enriched sea spray aerosols: Methods, mechanisms, and human exposure. *Environmental science & technology*, *55*(9), 6184–6196. https://doi.org/10.1021/acs.est.1c00995

van Pinxteren, M., Müller, C., Iinuma, Y., Stolle, C., & Herrmann, H. (2012). Chemical characterization of dissolved organic compounds from coastal sea surface microlayers (Baltic Sea, Germany). *Environmental science & technology*, *46*(19), 10455-10462. https://doi.org/10.1021/es204492b

Van Pinxteren, M., Barthel, S., Fomba, K. W., Müller, K., Von Tümpling, W., & Herrmann, H. (2017). The influence of environmental drivers on the enrichment of organic carbon in the sea surface microlayer and in submicron aerosol particles–measurements from the Atlantic Ocean. *Elementa: Science of the Anthropocene*, *5*, 35. https://doi.org/10.1525/elementa.225

Wang, X., Bolan, N., Tsang, D. C., Sarkar, B., Bradney, L., & Li, Y. (2021). A review of microplastics aggregation in aquatic environment: Influence factors, analytical methods, and environmental implications. *Journal of Hazardous Materials*, *402*, 123496. https://doi.org/10.1016/j.jhazmat.2020.123496

Wurl, O., & Holmes, M. (2008). The gelatinous nature of the sea-surface microlayer. *Marine Chemistry*, *110*(1-2), 89-97. https://doi.org/10.1016/j.marchem.2008.02.009

Yang, S., Zhang, T., Gan, Y., Lu, X., Chen, H., Chen, J., ... & Wang, X. (2022). Constraining microplastic particle emission flux from the ocean. *Environmental Science & Technology Letters*, *9*(6), 513-519. http://dx.doi.org/10.1021/acs.estlett.2c00214

651 Zimmermann, L.; Göttlich, S.; Oehlmann, J.; Wagner, M.; Völker, C. (2020) What are the drivers of
652 microplastic toxicity? Comparing the toxicity of plastic chemicals and particles to Daphnia
653 magna. *Environmental Pollution, 267*, 115392. https://doi.org/10.1016/j.envpol.2020.115392

Supporting information

A. Materials and methods

A.1 Installation experimental setup

The experimental setup used for mimicking the sea spray aerosol formation in the sea is based on the article of Masry et al. (2021). A schematic overview of the experimental setup can be seen in Figure A.1. A glass Weck jar of 2 L was used, filled with seawater and closed off with a lid with 1 small and 2 bigger openings in it. To avoid air escaping the installation via other ways than the openings, a rubber ring and clamps were used to better close off the Weck jar. On the bottom of the Weck jar, a cuboid oxygen stone (from Aqua Della, dimensions: 30*15*15mm) was pasted, using Tesa power strips. A smaller plastic tube (inner diameter 5mm, outer diameter 7mm) was placed through the smallest opening in the lid and connected the oxygen stone with the air supply.

Two stainless steel filter holders were each put vertically in a clamp attached to a stand. In each of the filter holders an underdrain disc was placed under the filter, as described in Van Acker et al. (2021b). In one of the two filter holders a quartz filter (Whatman QM-A quartz filters with a diameter of 47mm and a pore size of 2.2 μm, category number: 1851-047) was placed to analyze the sodium concentration, as a proxy for the volume of SSAs collected. In the other filter holder a cellulose nitrate filter was placed, to analyze the aerosolized plastics. Two thicker plastic tubes (inner diameter 7mm and outer diameter 10mm) were put through the bigger openings in the lid of the Weck jar and were connected to the upper side of the filter holders, using metal connector pieces and Teflon tape. The two pumps were connected to the lower side of the filter holders. In between the pumps and the filter holders, a bottle of dried silica was placed to avoid water coming into the pumps. When the air supply was turned on, bubbles were created in the Weck jar filled with seawater and SSAs could form. The pumps sucked air through the filters in the filter holders and the formed SSAs were collected onto the filters. The details of the experimental setup used for the different experiments (type of plastics, type of filter, seawater type, air supply, number of replicates and concentration of plastics) can be found in Table A.1.

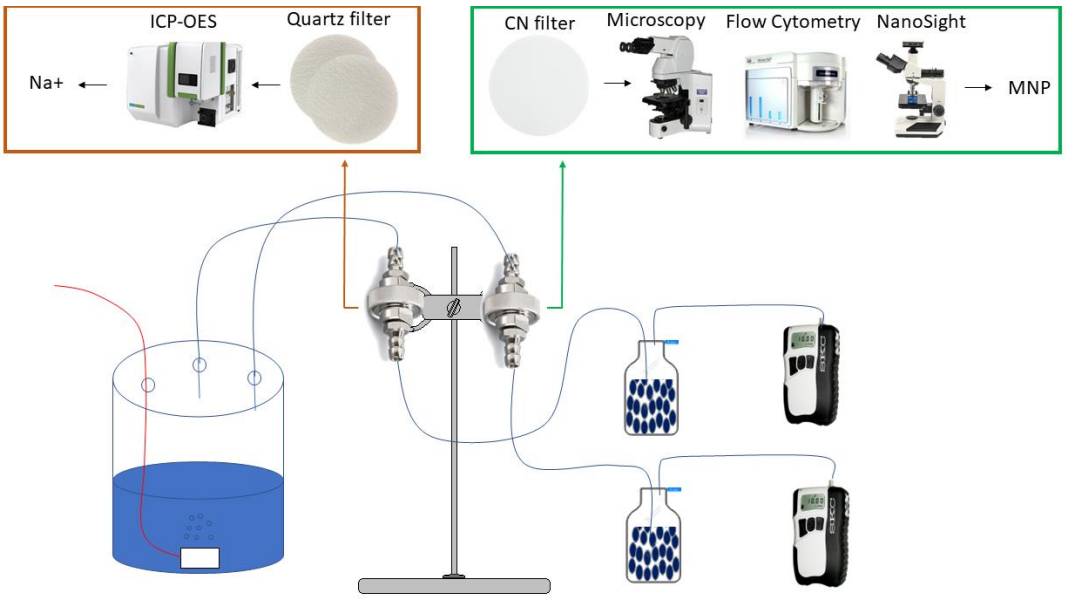

Figure A.1: Schematic overview of the experimental setup. The red line is air supply to the oxygen stone. The blue lines are the two thicker plastic tubes to connect to the filter holders. After the filter holders, the air goes through bottles filled with dry silica and at the end the pumps are connected.

683 *Table A.1: Experimental setup of the tests done in our study to investigate the influence of plastic size, type and*
684 *concentration and seawater characteristics on the aerosolization process. PE stands for polyethylene and TAF stands for*
685 *Thermoset amino formaldehyde. CN stands for cellulose nitrate. The experimental setup contained 800 mL of seawater.*

Series	Effect	Polymer	Size (µm)	Density (g/cm³)	Fluore-scent	number of plastics added	Supplier	Repli-cates	Seawater type	Pore size of CN filters (µm)	Air supply (L/min)
1	Size	PE	22-27	0.995	red	10^6	Cospheric UVPMS-BR 0.995	3	offshore	0.8	10
		PE	0.74-4.99	0.980	no	10^4	Cospheric PENS-0.98 740-499nm	3	offshore	0.8	10
		PE	Mostly <1	0.980	green	10^6	Cospheric Fluo green milled PE, provided by JRC	3	near shore filtered + coastal (pier)	0.2	5
2	Polymer type	PE	0.74-4.99	0.980	no	10^4	Cospheric PENS-0.98 740-499nm	3	offshore	0.8	10
		TAF	1-5	1.300	red	10^6	Cospheric FMR-1.3	3	offshore	0.8	10
3	Concentration	TAF	1-5	1.300	red	10^9	Cospheric FMR-1.3	2	offshore	0.8	10
4	Seawater type	TAF	1-5	1.300	red	10^9	Cospheric FMR-1.3	1	coastal (beach)	0.8	10

686

687 ## A.2 Validation of experimental setup

688 The experimental setup used was validated and believed to be suitable to study aerosolization of MNPs in a
689 controlled way, based on different parameters. This section elaborates on the validation of the experimental
690 setup. Sometimes little changes to the experimental setup were made to perform the validation of certain
691 aspects of the setup better, these are mentioned per validation experiment.
692
693 **SSA accumulation**
694 The experimental setup described above was validated to see if the SSAs are indeed collected on the filter. The
695 experiment ran with seawater (without any plastics added) for 24h with 2 quartz filters. Two pumps were used,

each set at a flow of 5 L/min, and the air was supplied at 10 L/min. The sodium was extracted from the quartz filters and a blank quartz filter was extracted together with the filters.

As it was confirmed that SSAs were collected onto the filter, next, it was validated if the sodium concentration collected on the quartz filter keeps increasing with increasing sampling time (as would be expected). For these experiments, only one pump was used and two quartz filters were put in parallel. The pump was set at 5L/min, so it was assumed 2.5L/min went through each filter holder. Filters were taken out after 4h, 8h, 11h, 16h, 20h and 24h. The sodium was extracted from the quartz filter.

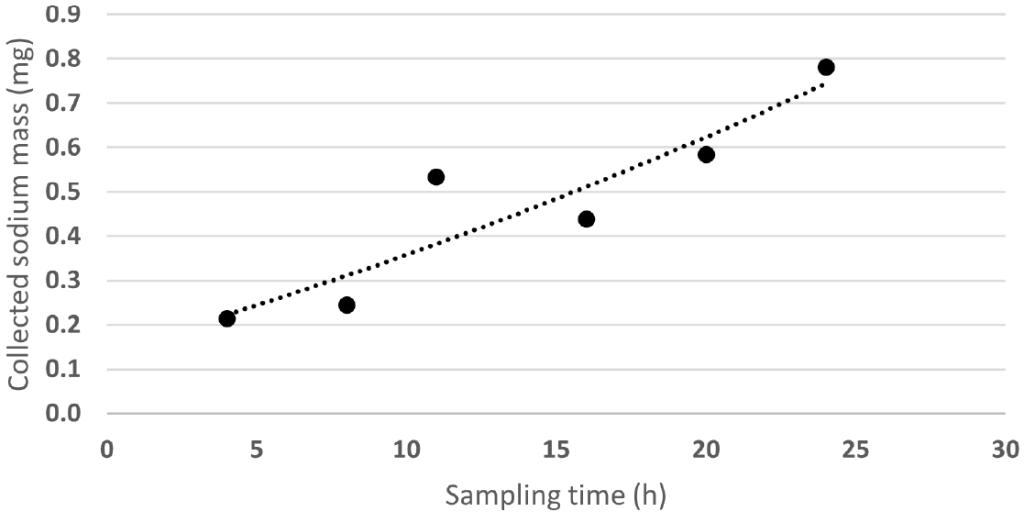

Figure A.2: The sodium concentration collected onto quartz filters relative to the air sampling time. It can be seen that the longer the experiment ran, the higher the collected sodium concentration is.

The results of the sodium concentration collected onto the quartz filters show a continuously increasing trend of the sodium concentration relative to the sampling time, except for the sample taken after 11 hours (Figure A.2). Due to practical limitations, the sample taken after 11 hours could only be extracted the next day while the other samples were always extracted immediately. Without the sample of 11 hours included, the coefficient of determination is 0.94. The regression line fits the observed data well. This shows a good quartz filter suitability for the collection, extraction and quantification of aerosolized Na^+ and thus SSAs. This corresponds to previous research by Van Acker et al. (2021b), which also found a good linearity ($R^2 > 0.90$) for the collected Na^+ on the quartz filter as a function of the sampling time.

Realistic bubble formation

It was also validated if the experimental setup mimics the bubble bursting process in the ocean as closely as possible and thus produces both film and jet drops. This was done by taking pictures of the bubbles created by the experimental setup. The glass Weck jar contained 800 mL of natural seawater. A black background was installed and pictures were taken of the bubbles in the water column. The camera used was a Canon EOS 750D equipped with a 250mm zoom lens with following settings: the focal length was 208 mm, the ISO value was ISO-3200, the F stop was f/5.6 and the exposure time was 1/2000 sec. Air was supplied at two different flow rates (5L/min and <2L/min) to see the difference in bubble size distribution. No pictures were taken at 10 L/min as it was too hard to differentiate and measure the bubbles. The lower the flow that was supplied, the fewer bubbles that were created and the easier it was to measure the bubbles. The airflow was measured using a rotameter of SKC, Inc. with a flow range between 2 and 26 L/min. All pictures taken were analyzed using Image J. The distinguishable bubbles were manually selected and their diameter was measured resulting in a bubble size distribution.

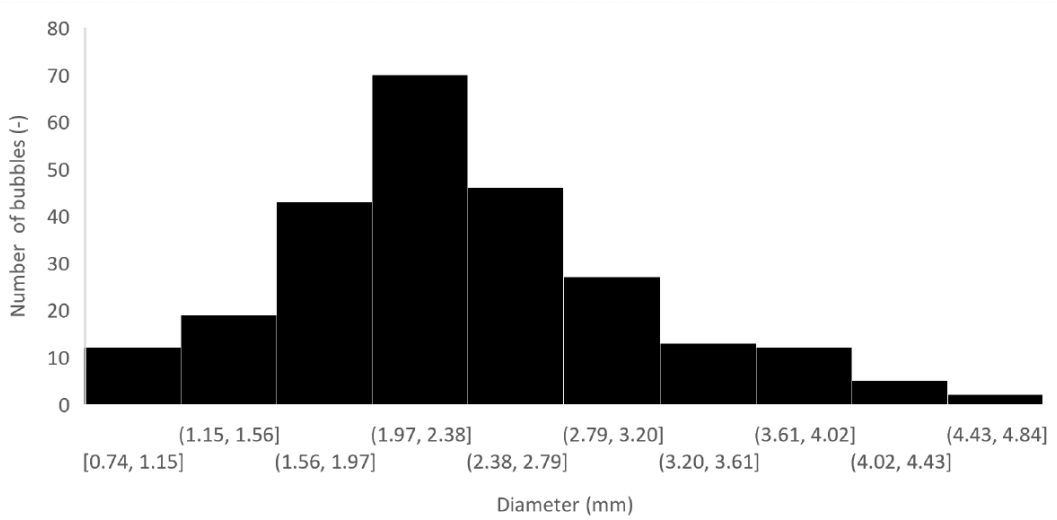

Figure A.3: The distribution of the bubbles formed at an air supply of 5L/min: the number of bubbles in function of the diameter of the bubbles in mm.

The bubble size distribution is centered around 2 mm in diameter, thus 1 mm in radius (Figure A.3). This size distribution is based on the bubbles formed when supplying 5 L/min of air to the experimental setup. The minimum bubble size measured is 0.74 mm diameter and the maximum bubble size measured is 4.84 mm diameter. A suitable estimate for the Hinze scale is about 1 mm in radius according to Deane and Stokes (2002). Film drops are produced by bubbles larger than the Hinze scale, whereas jet drops are produced in quantities greater than 1 per bubble by bubbles with a radius of less than 1.5 mm (Lewis et al., 2004; Stokes et al., 2013). Due to the broad size range of bubbles produced in our experimental setup (ranging between 0.37 mm radius and 2.42 mm radius) both film and jet drops will thus be produced creating a comparable situation to the sea. To conclude, the bubble bursting technique thus seems adequate to study the behavior of the bubbles and to generate a number of both film and jet drops, capable of producing SSA particles. This was also concluded in the study of Lv et al. (2020).

In the experiments mostly 10 L/min of air is supplied instead of 5 L/min. This may give different results in bubble size distribution compared to the results shown at 5L/min, but could not be measured as the bubbles were not clearly distinguishable on the images. Fuentes et al. (2010) did experiments with an aquarium diffuser with an aeration flow of 7.6, 8.1 and 8.5 L/min. The three bubble size distributions showed a difference in the bubbles created with a diameter smaller than 100 μm: the higher the aeration flow, the fewer bubbles with a diameter smaller than 100 μm were produced. We could not measure these very small bubbles in our experiment, our size distribution could thus only start at 0,74 mm diameter. For the bubbles with a diameter bigger than 100 µm, almost no difference was noticeable between the three bubble size distributions at the different airflows. The size distributions of Fuentes et al. (2010) stop at 1 mm, while ours only starts at 0,74 mm, however, the results of the study do show that no big differences are noticeable between the different airflows. With our experimental setup, validation experiments were also performed with an airflow lower than 2 L/min. This bubble size distribution did not differ a lot from the size distribution at 5 L/min. We thus suggest that there will not be too big of a difference between the bubble size distribution at 5L/min and 10L/min.

A.3 Validation of plastics

The polymer type, size and shape of the plastics used, were validated.

Polymer type

Infrared spectra were obtained using Attenuated Total Reflectance – Fourier Transformation infrared spectroscopy (ATR-FTIR) equipped with a diamond ATR Crystal (Thermo Fisher, Nicolet iz10). Three spectra were obtained and an average spectra was calculated using Omnic-software (Thermo Scientific, Version 2020). The spectra were uploaded in the OMNIC Anywhere, the online application provided by ThermoFisher, for further analysis. Spectra were compared to the Hummel Polymer Sample Library to estimate the spectral match between the obtained spectrum and the expected spectrum present in the library.

1) PE mostly <1µm, dissolved in a solution of methanol and triton.

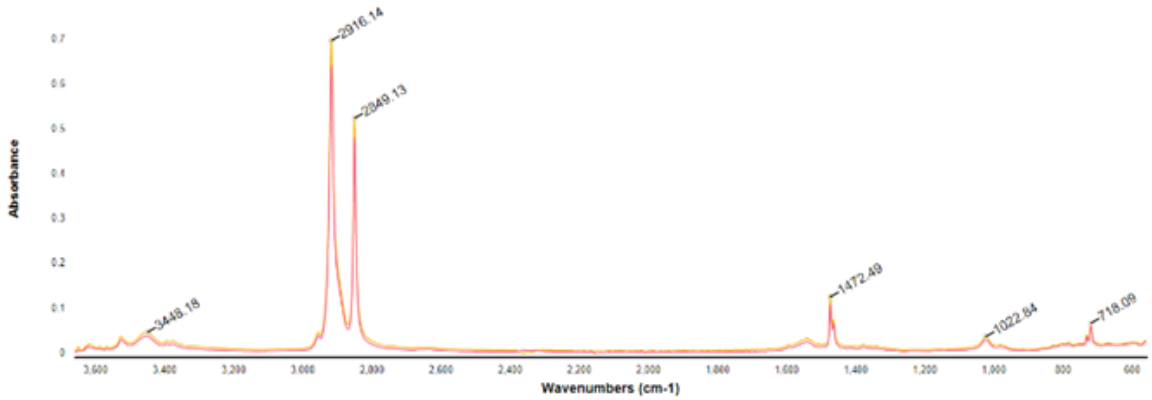

Figure A.4: ATR-FTIR spectrum of PE mostly <1µm particles, dissolved in a solution of methanol and triton.

No spectral match with the Hummel Polymer Sample Library could be estimated as the plastics are dissolved in a solution of methanol and triton. However, as also seen in the PE spectra below, peaks can be seen around 2920 and 2850 cm-1, characteristic for stretching of CH2 bonds present in PE (Figure A.4).

2) PE 0.74-4.99µm

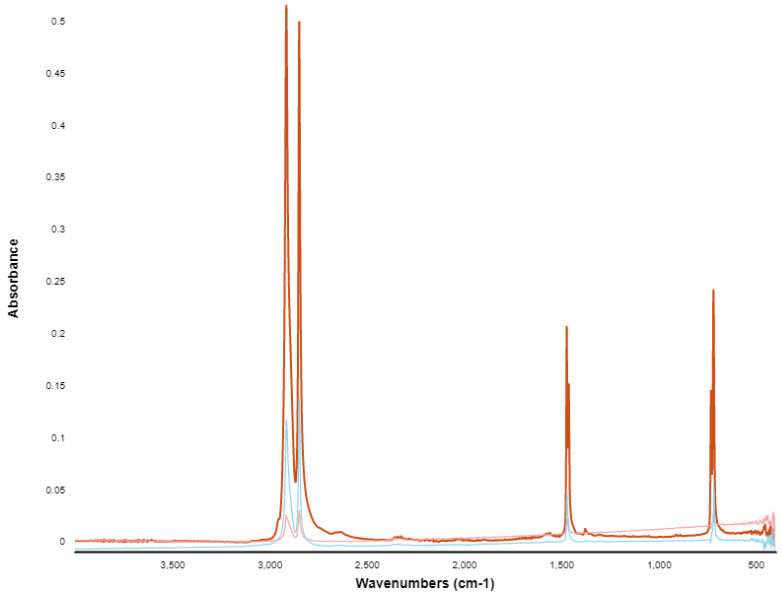

Figure A.5: ATR-FTIR spectrum of PE particles between 0.74 and 4.99µm.

The ATR-FTIR spectrum in Figure A.5 shows peaks around 2920 and 2850 cm-1, characteristic for stretching of CH2 bonds present in PE. The spectrum matches with the polyethylene spectrum present in the Hummel Polymer Sample Library with a match percentage of 63.75%.

3) PE 22-27µm

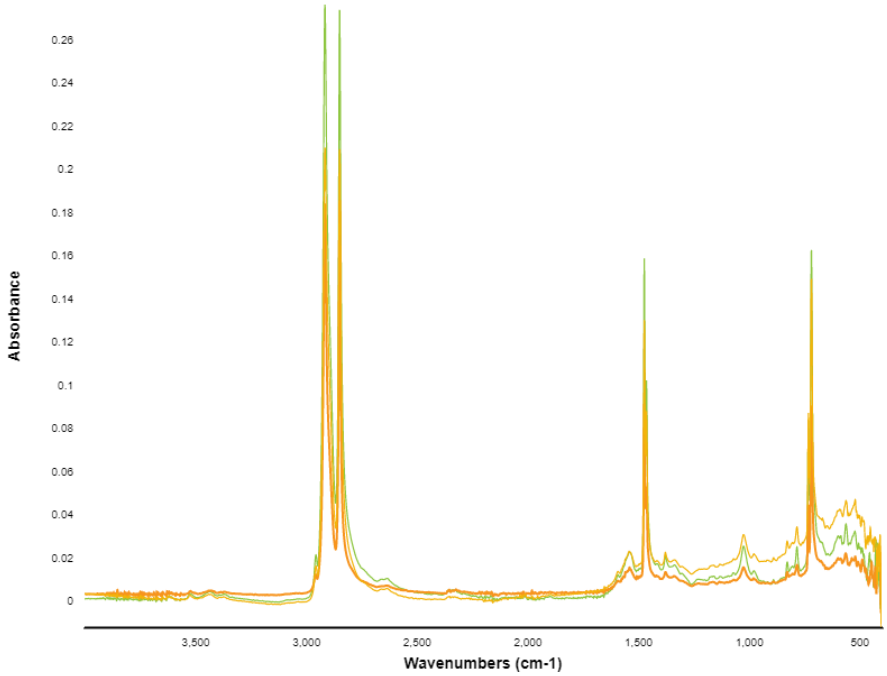

Figure A.6: ATR-FTIR spectrum of PE particles between 22 and 27µm.

The ATR-FTIR spectrum in Figure A.6 shows peaks around 2920 and 2850 cm-1, characteristic for stretching of CH2 bonds present in PE. The spectrum matches with the polyethylene spectrum present in the Hummel Polymer Sample Library with a match percentage of 66.03%.

4) TAF 1-5µm

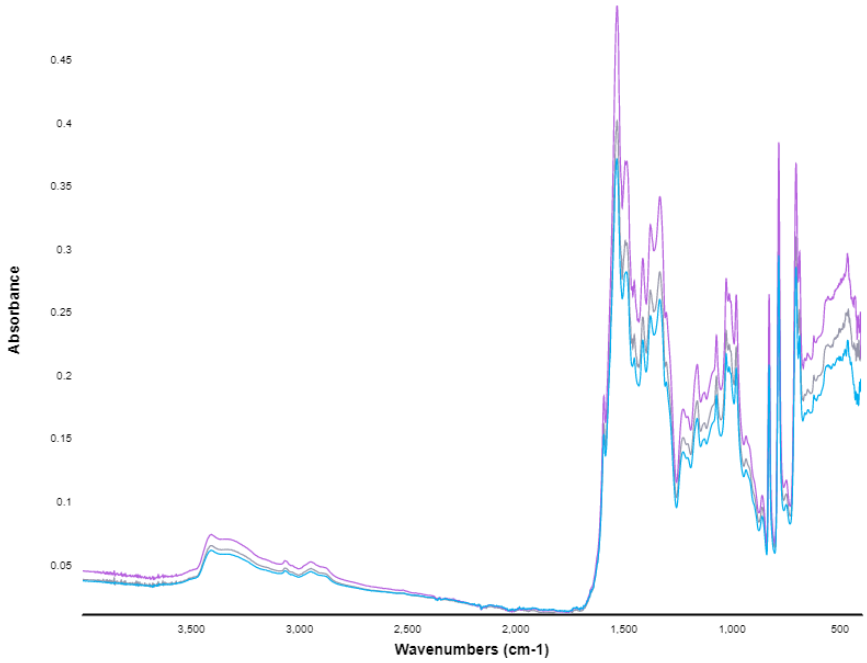

Figure A.7: ATR-FTIR spectrum of TAF particles between 1 and 5µm.

Thermoset amino formaldehyde does not match with a known polymer in the Hummel Polymer Sample Library. The supplier also does not mention a spectrum. However, the spectrum obtained with the ATR-FTIR clearly shows that this polymer is not PE (Figure A.7).

Size

Pictures were taken with the BX41 Olympus microscope and Olympus cellSens Dimension 1.18 software. The Olympus UC30 camera (U-TV0.5XC-3) was connected to the microscope. The particles on the pictures were then measured using image J. Fifty particles of each plastic type were measured to derive a size distribution.

Table A.2: Size measurements of the plastics used in the experiments. Column 2 and 3 show the nominal size that was mentioned by the supplier. Column 4, 5 and 6 show the measured minimum, maximum and average size of the particles.

plastic type	nominal minimum size (µm)	nominal maximum size (µm)	measured minimum size (µm)	measured maximum size (µm)	measured mean size (µm)
Cospheric PENS-0.98 740-499nm	0.74	4.99	1.73	4.83	3.13
Cospheric UVPMS-BR 0.995	22	27	20.01	26.91	23.97
Cospheric FMR-1.3	1	5	1.04	4.83	2.71

The measurements (Table A.2) approximately confirm the nominal sizes, except for the Cospheric PENS-0.98 740-499 nm. However, the fact that the smallest particle measured is only 1.73 is due to the technical difficulties to measure smaller particles under this microscope. The nanoplastics are thus measured using a different technique namely the nanoparticle tracking analysis. A Nanosight from the brand Malvern type LM10 with the NTA 3.0 software was used. The size distribution that resulted from the Nanosight (Figure A.8), showed that the plastic solutions indeed contains all sizes of plastics lower than 5 µm. Besides, it indicates that the biggest share of plastic particles has a diameter smaller than 1 µm.

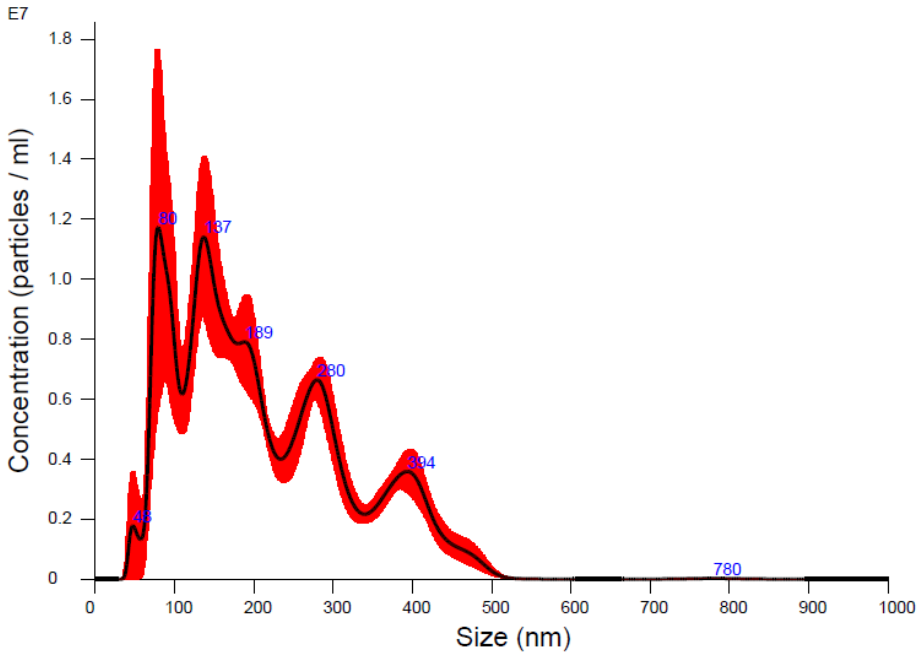

Figure A.8: Size distribution of the PE mostly <1µm solution, measured with the Nanosight.

Shape

To validate the shape, pictures were taken with the scanning electron microscope Phenom ProX Desktop at VLIZ (Ostend, Belgium).

1) PE nanoparticles

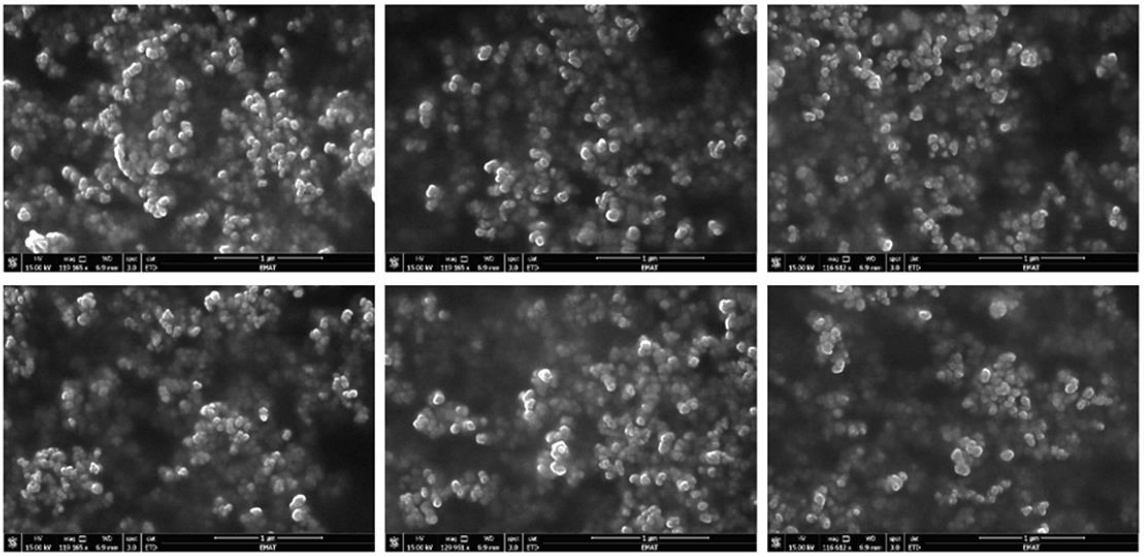

Figure A.9: SEM image of the PE nanoparticles.

The pictures of the SEM (Figure A.9) show the spherical shape of the particles.

2) PE 0.74-4.99 µm

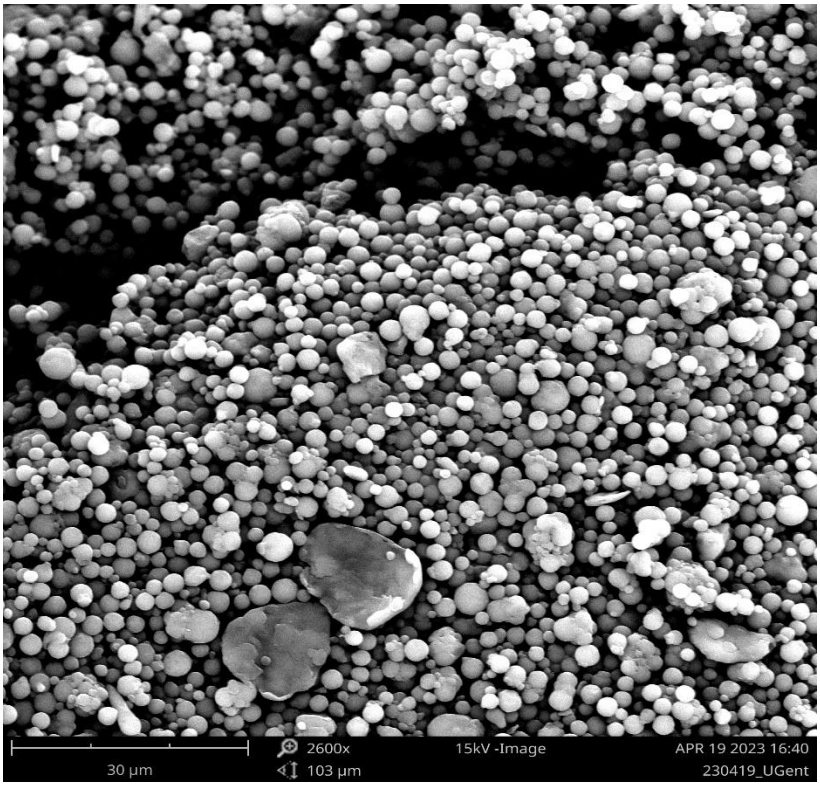

Figure A.10: SEM image of the PE particles between 0.74 and 4.99µm.

Figure A.10 shows that the PE particles between 0.74 and 4.99 µm are not all spherical.

3) PE 22-27 µm

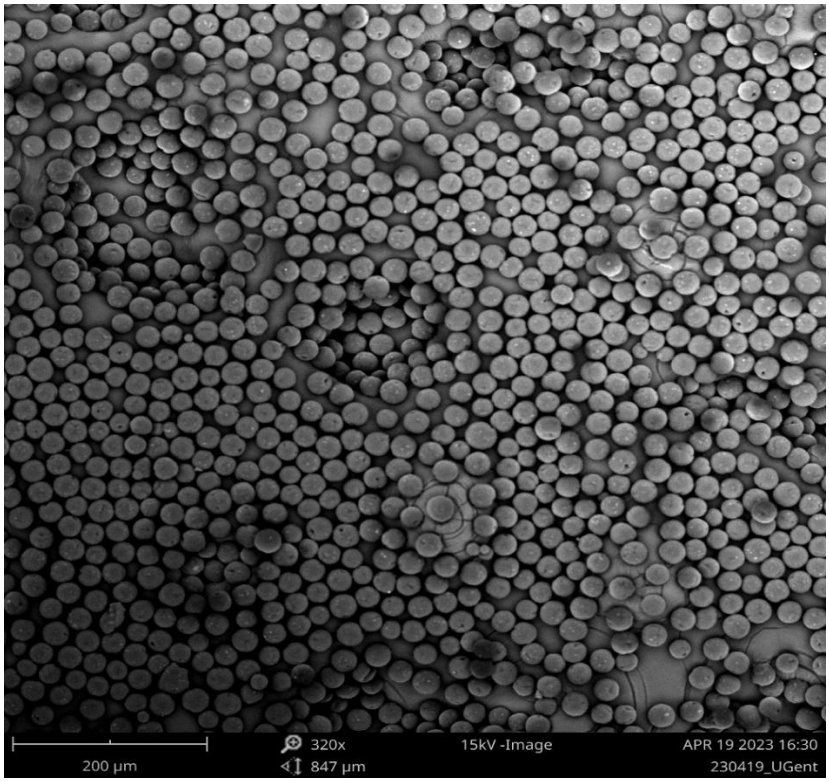

Figure A.11: SEM image of PE particles between 22 and 27 µm.

Figure A.11 shows the spherical shape of the PE particles between 22 and 27 µm.

4) TAF 1-5 µm

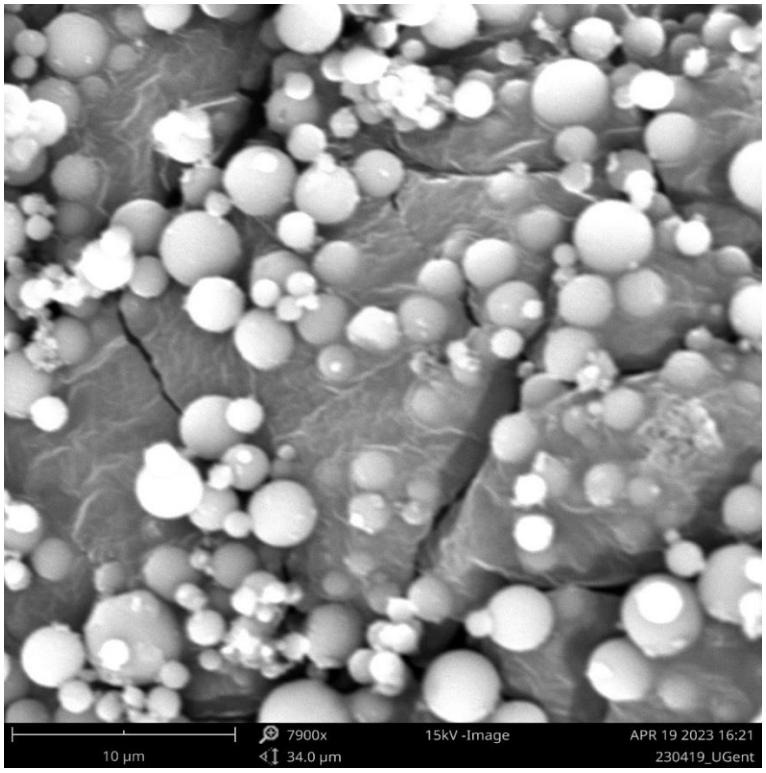

Figure A.12: SEM image of TAF particles between 1 and 5 µm.

Figure A.12 shows the spherical shape of the TAF particles between 1 and 5 µm.

A.4 Extraction and analysis of microplastics

The preparation steps happening with the samples before analysis, could result in a loss of plastics. However, while being transferred from recipient to recipient, the recipient was always rinsed 3 times to try to avoid this from happening.

PE particles 22-27µm: microscopic analysis

Under the microscope, the cellulose nitrate filters could be directly analyzed, no pre-treatment steps were needed. The number of plastics was analyzed using the BX41 Olympus microscope and Olympus cellSens Dimension 1.18 software. Pictures were taken of every part of the filter with the Olympus UC30 camera (U-TV0.5XC-3) connected to the microscope. The settings were: an exposure time of 20.6 msec and a gain of 2.7dB. The light intensity was the same for all images. The particles on the pictures were then counted using image J. A color threshold was set based on the red color of the microplastics in a control sample, distinguishing the plastic particles from the organic material and filter background. The filters of the blank experiments were also analyzed under the microscope and no plastics (that could be seen under the microscope) were found. The PE 22-27 µm are also colored and thus easily differentiated from the possible present plastics.

PE particles 0.74-4.99µm and TAF particles 1-5µm: Flow cytometry

For the flow cytometry, the cellulose nitrate filters needed to be digested before analysis. The filters were placed in glass beakers and 30 mL of 10 % KOH was added to the filters using a glass pipette. The beakers were placed in a hot water bath at 60°C for 24h to let the filters fully digest. As the pH of the KOH solution was too high for the flow cytometer, HCl was added with a glass pipette until neutral pH was reached in the samples. To avoid damage to the plastics, this was done immediately before flow cytometry measurements. As the flow cytometer can only analyze small volumes and high concentrations of particles, the samples were evaporated in the oven at 60°C. After complete evaporation, the samples were dissolved in around 2 mL of deionized water. Finally, the samples were filtered over 20 µm filters to remove all big salt crystals that could lead to obstruction of the flow cytometer. The seawater samples (5 or 10 mL) were also evaporated in the oven at 60°C and dissolved again in around 2 mL of deionized water to increase the concentrations for analysis with the flow cytometer.

The Attune NxT Flow Cytometer, from Invitrogen by Thermo Fisher Scientific, was used for the analysis. The combination of the Attune NxT Acoustic Focusing Cytometer with the Attune NxT autosampler was used. For the flow cytometry analysis, the wells of a 96 well plate with a flat bottom were each filled with 200 µL of sample. For each sample at least 3 wells were filled to have at least three replicate measurements. The flow cytometer always sucked up and measured around 100 µL of the 200 µL present in the well. The exact volume analyzed was extracted from the files in R studio and the count of microplastics per µL was calculated to account for these differences in volume analyzed.

The already fluorescent plastic particles did not need staining and were analyzed directly. The non-fluorescent particles were stained first with Bodipy. The Bodipy 496/503 (4,4-Difluoro-1,3,5,7,8-Pentamethyl-4-Bora-3a,4a-Diaza-s-Indacene) used, came from Invitrogen by Thermo Fischer Scientific (catalog code: D3922). A solution of 12.5 µg/mL of Bodipy dissolved in DMSO was created and 2 µL of this solution was added to each well filled with 200 µL of sample. The samples were then stored in the dark for 30 minutes before analysis, to let the stain react. Positive control and negative control samples were measured together with the other samples. Control samples with TAF particles were also filtered over a 20 µm filter to make sure that this filter step, used in the preparation of the cellulose nitrate filter samples, does not remove any microplastics. Blanks of the filter and seawater were also incorporated to take into account the background noise. During the measurement of the cellulose nitrate filter samples, the well plate was shaken in between the measurements to avoid sedimentation of the particles. No shaking happened during the analysis of the water samples.

As there was not a very clear pattern observable in the data of the flow cytometer, defining a gating set was hard. That's why another approach was used here. The mean value from the blank samples was subtracted from the results. This way other particles present in the seawater besides plastics are removed from the results and also the noise created by the cellulose nitrate filters themselves is subtracted. This then gives an indication of the number of microplastics present in the samples. It is important to note that more noise is expected in the samples with microplastic than in the blank samples and this is thus not taken into account when using this method. This method will thus not give a completely correct image. As microplastics are not spread homogeneously, this could result in variation between the replicates. The mean value of the counts per µL of all

replicates is calculated and used in the EF calculations. The limit of detection was calculated by following respectively Equations A.1. Only the values higher than the LOD were taken into account in the EF calculations. If the EF SSA of a replicate experiment could not be calculated because the number of particles was under the LOD, a sensitivity analysis was performed as follows: (1) this EF SSA value was excluded in the calculation of the mean EF SSA (2) this EF SSA value was seen as zero in the calculation of the mean EF SSA (3) the LOD value was used to calculate the EF SSA and this value was used in the calculation of the mean EF SSA.

$$LOD = mean_{blank} + 1.645 \times sigma_{blank} \quad \text{(Eq. A.1)}$$

PE nanoplastics: Nanosight

The nanoplastics on the cellulose nitrate filters and in the water samples were analyzed using nanoparticle tracking analysis. A Nanosight from the brand Malvern type LM10 with the NTA 3.0 software was used. The Nanosight can detect particles between 40 nm and 1 µm ideally in a concentration between 10^8 and 10^{10} particles per mL. The plastic stock solution used in the experiments contains all sizes of plastics lower than 5 µm, but the known size distribution of the stock solution (Figure A.8) indicates that the biggest share of plastic particles has a diameter smaller than 1 µm and can thus be analyzed using the Nanosight. This high concentration of nanoparticles was the reason the Nanosight was used instead of the flow cytometer for the analysis of these experiments.

The cellulose nitrate filters were dissolved in 30 mL of 10% KOH using a glass pipette and were placed in a warm water bath at 60°C for 24h to let the filters fully digest. For the water samples, no pretreatment was needed. For each measurement, one mL of the sample was sucked up with a plastic syringe. This syringe was then connected to the cell of the Nanosight to inject the sample for analysis. A laser is sent through the cell containing the sample. The samples were analyzed in fluorescence mode. The excitation wavelength in fluorescence mode was 488 nm. The detection threshold was set at five, the standard value of the Nanosight.

For each sample five replicate measurements were performed, each consisting of a video of 60 seconds. The syringe was pushed a little further every time so five different volumes of the same sample were measured. Based on these videos, five size distributions were generated that were combined into one general size distribution of each sample based on the mean and standard error of the five measurements. The recording time was set at one minute because in the manual of the Nanosight this is recommended. A sample of the stock solution of the plastic particles was also analyzed with the Nanosight as a control.

To validate the reliability of the results, a second measurement was done of the samples of one replicate experiment. A lot of different options were tested in scattering mode to find the ideal settings for the analysis of these heterogeneous samples. The number of videos taken from each sample and the duration of each video were adjusted during the different tests. Based on all these tests, it was concluded that for each sample three videos of three minutes were the best settings instead of 5 videos of 1 minute. The samples themselves were measured in fluorescence mode instead of scattering mode to try to only count the fluorescent plastic particles.

When looking in detail at the videos of the blank experiment samples, no green fluorescent plastic particles were found. However, the results of the nanoparticle tracking analysis show a lot of background noise that is measured as particles as the concentration in the sample is too low for the Nanosight. This is because the Nanosight keeps looking for particles when it cannot find strong fluorescent ones. The information accompanying the results of the measurements also tells us noise is measured in all five replicate measurements of each of the blank experiment samples. This noise measurement in the blank experiment samples could not be corrected for in our results. However, for the EF calculations the assumption is made that the same noise is measured in the filter and water samples and that by dividing these measurements, the noise is taken into account.

A.5 Quantification of production of sea spray aerosols

The filter holder was disconnected from the pumps and kept in alumina foil until extraction, to avoid contamination. The quartz filter was taken out of the filter holder and the sodium was extracted immediately. One-quarter of the quartz filter was used for the quantification of the sodium concentration and was placed in a falcon tube. A picture of the remaining three-quarters of the filter was taken to correct later for the exact surface area that was analyzed for the sodium content. Using a glass pipette, 5 mL of 1% HNO_3 was added to the

falcon tube and vortexed for 20 seconds. The sample was then sonicated for five minutes after which the supernatant was transferred to a new 15 mL falcon tube. The step of adding 5 mL of 1% HNO_3, vortex and sonicate was repeated three times. Then, 1% of HNO_3 was added until a total volume of 15 mL was reached in the falcon tube and. The supernatant was mixed and transferred to a 20 mL syringe equipped with a Supor 0.45 µm filter. The Supor filter was first rinsed with ± 3mL supernatants (=waste). Then, ± 12 mL of the supernatant was transferred into an AAS tube.

The sodium was also removed from the filter holder itself as Van Acker et al. (2021b) showed that the filter holder contains a big part of the sodium collected. The filter holder was rinsed six times with 5 mL 1% *HNO_3*, this was collected in two 15 mL falcon tubes. Subsequently, the same protocol as described above was used.

Next to the sodium content on the filters, the sodium content of the water samples was analyzed. The water samples were first transferred to a 20 mL syringe equipped with a Supor 0.45µ.m filter to remove the plastics. The Supor filter was first rinsed with ± 3mL supernatants (=waste). Then, ± 12 mL of the supernatant was transferred into an AAS tube. The samples were then 200 times diluted, as the concentration in the seawater samples was too high to be analyzed.

All samples were stored in the refrigerator until analysis with the inductively coupled plasma - optical emission spectrometer (ICP-OES) (iCAP 7200 of Thermo Fisher Scientific; LOD = 30 μg/mL; LOQ = 100 μg/mL). As a control for the sodium samples, blank quartz filters were extracted and analyzed together with the used filters. Samples of the reagent (1% HNO_3 solution) used in the extraction protocol were also taken, to account for background sodium concentration due to the used reagent.

B. Results

B.1. Enrichment factors

Table B.1 shows the results of the aerosolization experiments.

Table B.1: This table shows the results of the aerosolization experiments: the number of plastics in the air, in the surface water and in the bulk water, accompanied by the sodium concentration in the air.

Series	Plastic	Replicate experiment	Plastic particles per m³ air	plastic particles /mL surface water	plastic particles /mL bulk water	Sodium on filter (mg) per m³ air
1	PE 22-27µm	1	0	NM	NM	0.132
		2	0	NM	NM	0.169
		3	0	NM	NM	0.159
	PE 0.74-4.99µm	1	4.50E+4	<LOD	6.12E+4	0.068
		2	3.97E+4	<LOD	6.59E+4	0.065
		3	<LOD	<LOD	6.78E+4	0.081
	PE <1µm	1	4.09E+8	3.16E+7	2.76E+7	0.078
		2	2.37E+8	2.61E+7	7.51E+6	0.170
		3	2.33E+8	4.38E+7	2.19E+7	0.069
2	TAF 1-5 µm lower concentrations	1	<LOD	9.55E+3	2.05E+3	0.067
		2	<LOD	7.45E+3	7.60E+3	0.089
		3	5.01E+4	6.93E+3	3.99E+3	0.063
3	TAF 1-5µm higher concentrations	1	1.79E+5	3.77E+4	3.57E+4	0.098
		2	8.04E+4	3.27E+4	2.60E+4	0.165
4	TAF 1-5µm coastal water	1	6.11E+5	4.83E+4	1.64E+4	0.324

The mean sodium concentration of all samples is 0,123 +/- 0,0677 mg sodium/ m^3 air (Table B.1). The minimum value is 0,063 mg sodium/ m^3 air and the maximum value is 0,324 mg sodium/ m^3 air: a lot of variation can thus be seen between the experiments. Looking more specifically at the results, it is seen that the origin of the seawater used in the experiments has an effect on the measured sodium concentration: the filters of the coastal seawater experiment has a much higher collected sodium mass than the other filters. Most experiments were done with seawater from the same barrel of offshore seawater: here a decreasing trend in sodium concentration relative to time is visible. For the experiments with the PE nanoplastics again different seawater was used.

Due to technical implications the sodium concentration in the water samples was only measured in a subset of samples. Most experiments were performed with seawater from the same barrel of offshore seawater. The results of the subset of samples seem similar and thus the mean values of the results of these experiments are used in further calculations as the sodium concentration for all water samples, namely 1.02E+4 +/- 1.97E+2 for the surface water and 1.00E+4 +/- 2.03E+2 for the water column sample. The experiments with the nanoplastics were performed with different seawater, the mean value for the surface water was 1.12 +/- 2.51E+2 and for the water column 1.12 +/- 1.53E+2.

No PE particles of the biggest tested size, 22-27 µm, were found on the cellulose nitrate filters under the microscope, indicating that these particles seem too big to be aerosolized in our experiments. After the experiments, plastics were found at the side of the glass Weck jar around 5 cm above the water surface. This is due to the bursting of the bubbles against the sides and the plastics sticking at the sides. With the unaided eye, no plastics were seen higher than 5 cm above the water surface and no plastics were seen in the tubes. The microscope also showed no particles on the filters. So based on these observations, it can be concluded that these PE particles with a size of 22-27 µm did not get into the air in our experiments, although limited transport via the bubbles might be possible.

The size distributions of the nanoplastics on the filters and in the water samples can be found in Figure B.1. A clear shift in size distribution is visible between the filter and water samples. In the surface samples, bigger and smaller particles are found, but the biggest share is the smaller particles. In the water column samples bigger particles can be found more than in the surface samples. On the filters almost only the smallest particles were detected, the biggest share of particles is smaller than 300 nm.

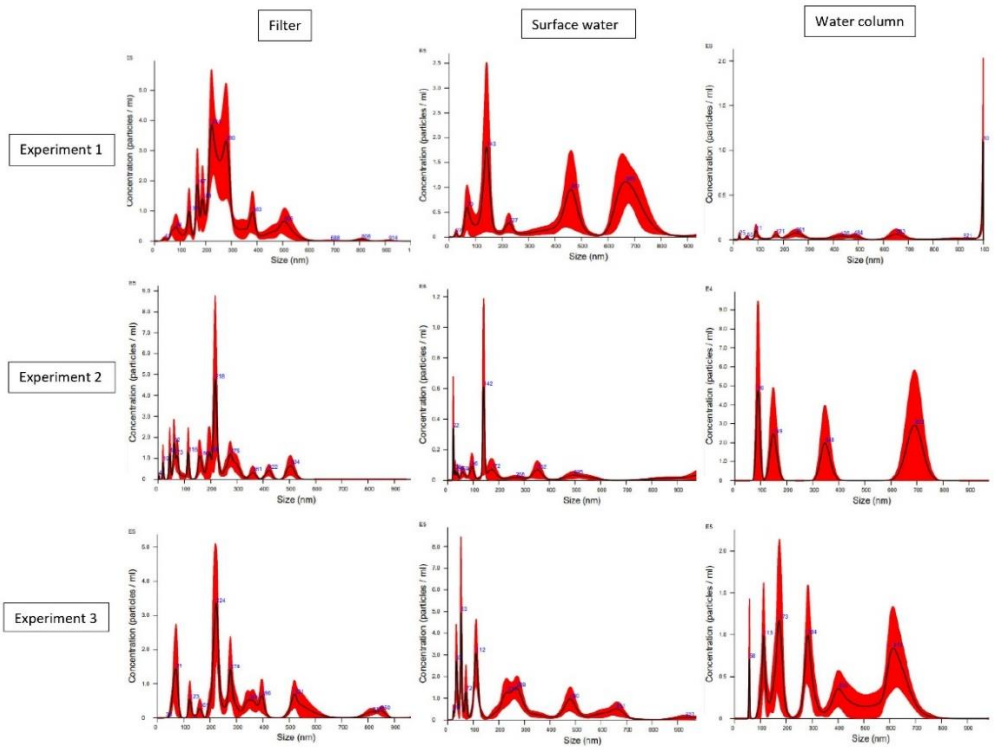

Figure B.1: This figure shows the size distributions (given by the Nanosight) for the three replicate experiments with the nanoparticles. The first column shows the size distribution of the plastics in the air, the second of the plastics in the surface water and third of the plastics in the water column samples.

Tables B.2, 3, 4 and 5 show the raw data of the flow cytometer, the blank measurements and LODs.

Filters PE 0.74-4.99 µm:

Table B.2: This table shows the raw data of the filters of the experiments with PE 0.74-4.99 µm particles. The table gives the counts, the counts per µl (taken into account the specific volume analyzed by the flow cytometer) and the final results after subtraction of the blanks to take into account background particles. The values in red are the values below the LOD.

sample	count	count per µL	count per µL minus blank
blank	11184	138,0741	
blank	12939	157,7927	
blank	11919	148,9875	
mean blank	**12014**	**148,2848 +/- 9,87807**	
1	18329	223,5244	75,23964
1	18989	231,5732	83,28842
1	20029	244,2561	95,97135
1	17878	218,0244	69,73964
mean of 1	**18806**	**229,3445 +/- 11,39212**	**81,05976**
2	16586	207,325	59,04025
2	15749	192,061	43,77622
2	18555	226,2805	77,99574
2	16925	206,4024	58,11769
mean of 2	**16954**	**208,0172 +/- 14,03846**	**59,73247**
3	13033	158,939	10,65427
3	10666	130,0732	-18,2116
3	10840	133,8272	-14,4576
3	10906	133	-15,2848

Mean of 3	**11361**	**138,9598 +/- 13,41646**	**-9,32491**

LOD= mean(11184,12939,11919) + 1.645 * 881.3484 = 13463.82

Filters TAF 1-5 µm:

Table B.3: This table shows the raw data of the filters of the experiments with TAF 1-5 µm particles. The table gives the counts, the counts per µl (taken into account the specific volume analyzed by the flow cytometer) and the final results after subtraction of the blanks to take into account background particles. The values in red are the values below the LOD.

sample	count	count per µL	count per µL minus blank
blank	8307	102,5556	
blank	9031	110,1341	
blank	7852	96,93827	
mean blank	**8397**	**103,2093 +/- 6,622185**	
Low conc 1	2068	25,85	-77,3593
Low conc 1	3333	43,85526	-59,3541
Low conc 1	3741	46,18519	-57,0241
Low conc 1	3274	32,74	-70,4693
Low conc 1	3160	39,5	-63,7093
mean of Low conc 1	**3115**	**37,62609**	**-65,5832**
Low conc 2	7653	93,32927	-9,88006
Low conc 2	8325	104,0625	0,853175
Low conc 2	7867	95,93902	-7,2703
Low conc 2	7996	99,95	-3,25932
Low conc 2	7913	98,9125	-4,29682
mean of Low conc 2	**7951**	**98,43866**	**-4,77067**
Low conc 3	16375	199,6951	96,4858
Low conc 3	15526	189,3415	86,13214
Low conc 3	13835	168,7195	65,51019
Low conc 3	13929	174,1125	70,90318
Low conc 3	13820	170,6173	67,40796
mean of Low conc 3	**14697**	**180,4972 +/- 13,45244**	**77,28785**
Coastal water	78439	956,5732	853,3638
Coastal water	85137	1038,256	935,0468
Coastal water	85268	1065,85	962,6407
Coastal water	78754	972,2716	869,0623
Coastal water	76493	932,8415	829,6321
mean of coastal water *	**80818**	**993,1585 +/- 56,41529**	**889,9491**
High conc 1	25042	313,025	209,8157
High conc 1	24320	304	200,7907
High conc 1	25958	324,475	221,2657
High conc 1	28098	342,6585	239,4492
High conc 1	25922	324,025	220,8157
mean of High conc 1	**25868**	**321,6367 +/- 14,49907**	**218,4274**
High conc 2	18629	229,9877	126,7783
High conc 2	17542	219,275	116,0657
High conc 2	16350	204,375	101,1657
High conc 2	18062	220,2683	117,059

High conc 2	18312	223,3171	120,1077
mean of High conc 2	**17779**	**219,4446 +/- 9,406808**	**116,2353**

* same blank is used as offshore water

LOD= mean(8307, 9031, 7852) + 1.645 * 594.59 = 9380.12

Water samples PE 0.74-4.99 µm:

Table B.4: This table shows the raw data of the water samples (surface and bulk) of the experiments with PE 0.74-4.99 µm particles. The table gives the counts, the counts per µl (taken into account the specific volume analyzed by the flow cytometer) and the final results after subtraction of the blanks to take into account background particles. The values in red are the values below the LOD.

sample	**count**	**count per µL**	**count per µL minus blank**
blank	3034	37	37
blank	3840	46,8292683	46,8292683
blank	4344	52,9756098	52,9756098
Mean blank	**3739,333333**	**45,60162602 +/- 8,0582477**	**45,601626**
1 surface	2013	24,5487805	-21,052846
1 surface	1913	23,3292683	-22,272358
1 surface	1990	24,2682927	-21,333333
Mean 1 surface	**1972**	**24,04878049 +/- 0,63870314**	**-21,552846**
1 bulk	28816	351,414634	305,813008
1 bulk	29947	374,3375	328,735874
1 bulk	29538	364,666667	319,065041
Mean 1 bulk	**29433,66667**	**363,4729336 +/- 11,5079622**	**317,871308**
2 surface	2975	37,1875	-8,414126
2 surface	2461	30,382716	-15,21891
2 surface	2563	31,2560976	-14,345528
Mean 2 surface	**2666,333333**	**32,94210454 +/- 3,70246348**	**-12,659521**
2 bulk	30777	375,329268	329,727642
2 bulk	30679	374,134146	328,53252
2 bulk	32919	411,4875	365,885874
Mean 2 bulk	**31458,33333**	**386,9836382 +/- 21,2293785**	**341,382012**
3 surface	2288	27,902439	-17,699187
3 surface	2343	30,0384615	-15,563164
3 surface	2396	29,2195122	-16,382114
Mean 3 surface	**2342,333333**	**29,05347092 +/- 1,07764805**	**-16,548155**
3 bulk	30772	384,65	339,048374
3 bulk	28461	347,085366	301,48374
3 bulk	27982	349,775	304,173374
Mean 3 bulk	**29071,66667**	**360,5034553 +/- 20,954719**	**314,901829**

LOD= mean(3034, 3840, 4344) + 1.645 * 660.78= 4826.3

Water samples TAF 1-5 µm:

Table B.5: This table shows the raw data of the water samples (surface and bulk) of the experiments with TAF 1-5 µm particles. The table gives the counts, the counts per µl (taken into account the specific volume analyzed by the flow cytometer) and the final results after subtraction of the blanks to take into account background particles.

water sample	**count**	**count per µL**	**count per µL minus blank**
blank	16727	203,988	
blank	16787	204,72	
blank	16997	207,28	
mean blank	**16837**	**205,329 +/- 1,728957**	
Low conc 1 surface	18556	237,897	32,56817
Low conc 1 surface	18093	226,163	20,83323
Low conc 1 surface	18331	223,549	18,21951
Mean low conc 1 surface	**18327**	**229,203 +/- 7,642253**	
Low conc 1 bulk	17762	216,61	11,28049
Low conc 1 bulk	17698	215,829	10,5
Low conc 1 bulk	17567	214,232	8,902439
Mean Low conc 1 bulk	**17675**	**215,556 +/- 1,212193**	
Low conc 2 surface	18054	231,462	26,13227
Low conc 2 surface	17938	218,756	13,42683
Low conc 2 surface	18177	221,671	16,34146
Mean low conc 2 surface	**18056**	**223,963 +/- 6,655614**	
Low conc 2 bulk	19430	239,877	34,54727
Low conc 2 bulk	20366	248,366	43,03659
Low conc 2 bulk	19818	241,683	36,35366
Mean low conc 2 bulk	**19871**	**243,308 +/- 4,472004**	
Low conc 3 surface	17926	218,61	13,28049
Low conc 3 surface	18081	220,5	15,17073
Low conc 3 surface	18768	228,878	23,54878
Mean Low conc 3 surface	**18258**	**222,663 +/- 5,465079**	
Low conc 3 bulk	18226	227,825	22,49573
Low conc 3 bulk	18430	224,756	19,42683
Low conc 3 bulk	18302	223,195	17,86585

Mean Low conc 3 bulk	**18319**	**225,259 +/- 2,35551**	
Coastal water surface	25836	315,073	109,7439
Coastal water surface	27371	333,793	128,4634
Coastal water surface	27003	329,305	123,9756
Mean coastal water surface *	**26737**	**326,057 +/- 9,77328**	
Coastal water bulk	22569	282,113	76,78323
Coastal water bulk	23174	282,61	77,28049
Coastal water bulk	24129	297,889	92,55962
Mean coastal water bulk	**23291**	**287,537 +/- 8,968404**	
High conc 1 surface	23573	287,476	82,14634
High conc 1 surface	25735	313,841	108,5122
High conc 1 surface	24385	297,378	92,04878
Mean high conc 1 surface	**24564**	**299,565 +/- 13,31829**	
High conc 1 bulk	30446	385,392	180,0631
High conc 1 bulk	31090	379,146	173,8171
High conc 1 bulk	31761	387,329	182
Mean high conc 1 surface	**31099**	**383,956 +/- 4,276389**	
High conc 2 surface	23095	296,09	90,76048
High conc 2 surface	22921	279,524	74,19512
High conc 2 surface	23413	285,524	80,19512
Mean high conc 2 surface	**23143**	**287,046 +/- 8,386871**	
High conc 2 bulk	37414	473,595	268,2657
High conc 2 bulk	21938	267,537	62,20732
High conc 2 bulk	21659	264,134	58,80488
Mean high conc 2 bulk	**27004**	**335,0886 +/- 119,9621**	

* same blank is used as offshore water

LOD= 16837+ 1.645* 141,77= 17070,22

B.2. Estimation of human exposure via inhalation

To obtain the human exposure prediction, we used the results of the experiments and performed some recalculations in 3 steps:

1. Extrapolation of Plastics/SSA from the experiment to the environment
2. Estimation of daily inhalation of SSA

3. Calculation of daily inhalation of MPs via SSA

Step 1:

The results of our experiments were recalculated to obtain a number of plastics per µg of Na+ (proxy for aerosol) (1), based on the number of plastics and mass of Na+ on the filters. For this, the data of three replicate experiments with the high concentration TAF plastics with a size of 1-5 µm are used. The focus is on particles between 1 and 5 µm as plastics smaller than 5 µm have the potential to reach the lungs (Jabbal et al., 2017; Lipworth et al., 2014). Nanoplastics (<1µm) are excluded here given the lack of reported environmental concentrations. Table B.6 shows the results of the filters and the surface water samples.

Table B.6: Results from the experiments: (1) the number of plastics/µg aerosol found on the filter, and (2) the concentration of plastics in the surface layer samples of the experiments.

	(1) number of plastics /µg aerosol	(2) concentration in surface water lab (part/m³)
Experiment 1	1882,374316	1,74E+10
Experiment 2	1816,690072	5,1E+10
Experiment 3	488,3532298	2,59E+10
Average:	1395,805873	3,14E+10

Evidently, in order to make a relevant extrapolation, the microplastic concentration in the environment should be taken into account. The North sea plastic data from Everaert et al. (2020) from 2010 was used as a reference. However, as described by Kooi and Koelmans (2019), the plastic size distribution almost always follows a power law distribution with higher concentrations of smaller particles. It would thus lead to an erroneous extrapolation if we compare our experimental situation (2) (with particles between 1-5 µm) with the environmental data (1-5000 µm). To account for that, the environmental concentrations were rescaled (3) using the method described by Koelmans et al. (2020). Based on the reported alfa value of this power law function for plastic in marine surface waters (by Kooi et al., 2021), a correction factor was calculated with following formula:

$$CF = \frac{\int_{x_{1D}}^{x_{2D}} bx^{-a}}{\int_{x_{1M}}^{x_{2M}} bx^{-a}} = \frac{x_{2D}^{1-a} - x_{1D}^{1-a}}{x_{2M}^{1-a} - x_{1M}^{1-a}}$$

Which allows us to recalculate the concentration in the original size range (1-5000 µm) to a concentration in the size range that corresponds with our experimental setup (1-5 µm).

The rescaling with the formulas of Koelmans et al. (2020) and Kooi et al. (2021) resulted in 92.798% of the plastics with a size between 1 µm and 5 mm, have a size between 1 and 5 µm. This is not surprising as indeed the concentrations increase as the particles are smaller. This leads to an estimated average concentration of 18,78495966 plastics/ m³ in the environment in 2010 (Table B.7).

As it is predicted that the plastic concentrations in the ocean will keep increasing, the prediction by Everaert et al. (2021) of plastic concentration in the environment by 2050 and 2100 were also rescaled in a similar manner as described before to allow a prediction for the future (Table B.7).

Table B.7: the concentration of plastics in the surface layer of the North sea. The concentration reported by Everaert et al. (2021) and the rescaled concentrations.

	Reported average concentration in Everaert et al. (2021) (1-5000 µm) [plastics/m³]	(3) Rescaled average concentration (1-5 µm) [plastics/m³]
2010	20,24285624	18,78495966
2050	114,4703059	106,2261202

2100	456,5844482	423,7010992

Based on the number of plastics on the filter (1) and in the surface layer (2) in our experiments, an estimation could be made of the number of plastics that is expected on the filter in the field (4) based on the rescaled environmental surface concentrations of the North Sea (3). The factor difference between the environmental surface concentration and the experimental surface concentration, was used to go from particles on the filter in the experiments to the estimation of particles on the filters in the field. This way we made an estimation of the particles/µg aerosol in the field (4) for the three TAF experiments and the average of the three experiments (Table B.8). The average will be further used in calculations.

Table B.8: The extrapolation for the number of plastics in the aerosols in the field.

(4)	Experiment 1 [plastics/µg aerosol in field]	Experiment 2 [plastics/µg aerosol in field]	Experiment 3 [plastics/µg aerosol in field]	Average [plastics/µg aerosol in field]
2010	2,0322E-06	6,69146E-07	3,54197E-07	8,34151E-07
2050	1,14918E-05	3,78392E-06	2,00293E-06	4,717E-06
2100	4,5837E-05	1,50928E-05	7,98903E-06	1,88146E-05

Step 2:

To determine the number of microplastics that are inhaled by coastal populations, information is needed about the volume of SSAs in coastal air. Van Acker et al. (2021a) measured the Na+ concentrations, which can be used as proxy for the volume of SSA, in the air at the Belgian coast in a 1-year SSA sampling campaign (March 19 2018 - March 19 2019; 300m from the waterline). Based on these measurements, on average 1.8 (minimum: 0.4; maximum: 6.3) µg SSA/m³ is present in the coastal air along the Belgian coast.

An average inhalation rate of 20 m³ air/day was estimated based on Duarte-Davidson et al. (2001). Inhaling at the coast thus gives an inhalation of 8 to 126 µg of SSAs per day, with an average of 36 µg of SSAs per day (SSA rate) (5).

Step 3:

Based on all calculated results above, the inhaled microplastics per day at the coast (6) can be calculated using the following formula:

inhaled plastics [# plastics/day]=plastic in SSA [(# plastics)/(µg SSA)]*SSA rate [(µg SSA)/day] (meaning (6) = (4) * (5))

The average inhaled plastic (6) was calculated for the three timepoints (2010, 2050, 2100) with corresponding minimal and maximal values, based on the minimum and maximum SSA rate (Table B.9).

Table B.9: The number of plastics inhaled per day for three timepoints (2010, 2050, 2100).

(6)	2010	2050	2100
Minimum number of plastics inhaled /day	6,67321E-06	3,7736E-05	0,000150517
Maximum number of plastics inhaled /day	0,000105103	0,000594342	0,002370635
Average number of plastics inhaled /day	3,00294E-05	0,000169812	0,000677324

References

Deane, G. B. and Stokes, M. D. (2002). Scale dependence of bubble creation mechanisms in breaking waves. *Nature*, *418*, 839–844. https://doi.org/10.1038/nature00967

Duarte-Davidson, R., Courage, C., Rushton, L., & Levy, L. (2001). Benzene in the environment: an assessment of the potential risks to the health of the population. *Occupational and environmental medicine*, *58*(1), 2-13. https://doi.org/10.1136/oem.58.1.2

Everaert, G., De Rijcke, M., Lonneville, B., Janssen, C. R., Backhaus, T., Mees, J., ... & Vandegehuchte, M. B. (2020). Risks of floating microplastic in the global ocean. *Environmental Pollution*, *267*, 115499. https://doi.org/10.1016/j.envpol.2020.115499

Fuentes, E., Coe, H., Green, D., Leeuw, G. d., and McFiggans, G. (2010). Laboratorygenerated primary marine aerosol via bubble-bursting and atomization. *Atmospheric Measurement Techniques*, *3*(1), 141–162. https://doi.org/10.5194/amt-3-141-2010

Jabbal, S., Poli, G., & Lipworth, B. (2017). Does size really matter?: Relationship of particle size to lung deposition and exhaled fraction. *Journal of Allergy and Clinical Immunology*, *139*(6), 2013-2014. https://doi.org/10.1016/j.jaci.2016.11.036

Koelmans, A. A., Redondo-Hasselerharm, P. E., Mohamed Nor, N. H., & Kooi, M. (2020). Solving the nonalignment of methods and approaches used in microplastic research to consistently characterize risk. *Environmental science & technology*, *54*(19), 12307-12315. https://doi.org/10.1021/acs.est.0c02982

Kooi, M., & Koelmans, A. A. (2019). Simplifying microplastic via continuous probability distributions for size, shape, and density. *Environmental Science & Technology Letters*, *6*(9), 551-557. https://doi.org/10.1021/acs.estlett.9b00379

Kooi, M., Primpke, S., Mintenig, S. M., Lorenz, C., Gerdts, G., & Koelmans, A. A. (2021). Characterizing the multidimensionality of microplastics across environmental compartments. *Water Research*, *202*, 117429. https://doi.org/10.1016/j.watres.2021.117429

Lewis, E. R., & Schwartz, S. E. (2004). Sea salt aerosol production: mechanisms, methods, measurements, and models, volume 152. *American geophysical union*. ISBN: 978-0-875-90417-7

Lipworth, B., Manoharan, A., & Anderson, W. (2014). Unlocking the quiet zone: the small airway asthma phenotype. *The Lancet Respiratory Medicine*, *2*(6), 497-506. https://doi.org/10.1016/s2213-2600(14)70103-1

Lv, C., Tsona, N. T., and Du, L. (2020). Sea spray aerosol formation: results on the role of different parameters and organic concentrations from bubble bursting experiments. *Chemosphere*, *252*, 126456. https://doi.org/10.1016/j.chemosphere.2020.126456

Masry, M., Rossignol, S., Roussel, B. T., Bourgogne, D., Bussière, P.-O., R'mili, B., and Wong-Wah-Chung, P. (2021). Experimental evidence of plastic particles transfer at the water-air interface through bubble bursting. *Environmental Pollution*, *280*, 116949. https://doi.org/10.1016/j.envpol.2021.116949

Stokes, M., Deane, G., Prather, K., Bertram, T., Ruppel, M., Ryder, O., Brady, J., and Zhao, D. (2013). A marine aerosol reference tank system as a breaking wave analogue for the production of foam and

sea-spray aerosols. *Atmospheric Measurement Techniques*, *6*(4), 1085–1094. https://doi.org/10.5194/amt-6-1085-2013

Van Acker, E., De Rijcke, M., Liu, Z., Asselman, J., De Schamphelaere, K. A., Vanhaecke, L., and Janssen, C. R. (2021a). Sea spray aerosols contain the major component of human lung surfactant. *Environmental science & technology, 55*(23), 15989-16000. http://doi.org/10.1021/acs.est.1c04075

Van Acker, E., Huysman, S., De Rijcke, M., Asselman, J., De Schamphelaere, K. A., Vanhhaecke, L., and Janssen, C. R. (2021b). Phycotoxin-enriched sea spray aerosols: Methods, mechanisms, and human exposure. *Environmental science & technology*, *55*(9), 6184– 6196. https://doi.org/10.1021/acs.est.1c00995